THE ASTRONOMICAL JOURNAL VOLUME 90, NUMBER 11 NOVEMBER 1985

COLOR-MAGNITUDE DIAGRAMS FOR THREE DISTANT GLOBULAR CLUSTERS

J. G. COHEN
Palomar Observatory, California Institute of Technology, Pasadena, California 91125
Received 17 January 1985; revised 5 August 1985

ABSTRACT

Color-magnitude diagrams are presented for three distant galactic globular clusters (NGC 5466, NGC 6229, and NGC 7006). In each case the photometry reaches below the main-sequence turnoff; the ages deduced by comparison with stellar evolutionary isochrones are indistinguishable from those of the well-studied nearby clusters. The luminosity functions derived from computer-generated star counts complete to a well-defined limiting magnitude in selected fields support identical ages for the three clusters with maximum differences between NGC 5466 and NGC 6229 of 10% of the age, and between NGC 5466 and NGC 7006 of 25%. The previously published claims of an exceptionally bright turnoff for NGC 7006 are shown to be spurious. The horizontal branch of NGC 6629 is unusually red for its metallicity. Star counts and tidal radii are discussed for NGC 6229 and NGC 7006.

I. INTRODUCTION

The halo globular clusters are of interest in problems of the formation and chemical evolution of the Galaxy. While the abundances of the halo clusters can be determined by analyzing their integrated light (see, for example, Zinn 1980; or Frogel, Persson, and Cohen 1983) or the spectra of their brighter giants, it is much more difficult to obtain information about the age of these clusters. This requires photometry reaching the main sequence, which for the more distant clusters in the outer halo of the Galaxy has until recently been impossible. Furthermore, the outer halo clusters are the most compressed in linear scale, making crowding problems more severe. We present here color-magnitude diagrams for three of the more distant galactic globular clusters (NGC 5466, NGC 6229, and NGC 7006). In each case we have succeeded in reaching the turnoff. We demonstrate that an earlier claim of a very young age for NGC 7006 is spurious. The luminosity functions for the three clusters are discussed in Sec. III*b*, while the horizontal-branch morphology of these clusters in the outer galactic halo is discussed in Sec. III*c*. Star counts and tidal radii for two of the clusters are discussed in Sec. IV. A summary of our conclusions is given in Sec. V.

II. OBSERVATIONAL MATERIAL

a) Instrumental Magnitudes

Frames of three distant globulars (NGC 5466, 6229, and 7006) were obtained in August 1984, March 1985, and April 1985 on the 5 m Hale telescope at Palomar Observatory using the 4-Shooter (see Gunn *et al.* 1984). The scale of the 4-Shooter is 0.33 arcsec/pixel. The seeing at the zenith was slightly better than 1.0 arcsec and the sky was photometric in the first two observing runs. Several frames were taken of each cluster as listed in Table I through the *g* and *r* filters of the Thuan and Gunn (1976) system. The *g* and *r* magnitudes were calibrated using out-of-focus exposures of the bright Thuan-Gunn standards. Standard extinction coefficients for Palomar were used. Short exposures were taken to find guide stars, and all the longer exposures were guided. The central core of each cluster is hopelessly confused (except for NGC 5466), but in the outer parts there is little or no overlap of the stellar images. However, even the outer parts are too crowded for standard aperture photometry. The procedure adopted was to isolate several small (less than 2 arcmin on a side) regions free of cosmetic defects in the CCDs on the periphery of each cluster, where the crowding was tolerable. The locations of the fields with respect to the cluster centers are given in Table II, and the fields are shown in Figs. 1–3 [Plates 244–246] (made from the 600 s *g* frames). In each field, a star is overlaid with a cursor (a cross) whose location and magnitude is also listed in Table II.

A list of the point sources whose central pixel was brighter than a predetermined threshold level was compiled for each exposure of each of the small fields. Sources with any saturated pixels were eliminated. The sky level was chosen by sampling regions free of stars within each of the fields and was taken as constant within each region. The sum of the detected CCD counts in a 5×5 pixel box centered on the point-source maximum (minus 25 times the mean sky for the region) was used to calculate the "box magnitudes" for each object. A selection of ten well-isolated stars in each field was used to determine the magnitude difference between large-aperture photometry and the box magnitude defined above. In the most crowded regions, only seven well-isolated objects could be found. Because the seeing was good, this offset was in the best cases only 0.12 mag and in the worst case (NGC 5466, observed at a large airmass in August 1984) was 0.4 mag. The dispersion in this offset within a given field as

TABLE I. Frames of NGC 5466, NGC 6229, and NGC 7006.

Object	*g* (s)	*r* (s)
NGC 5466	40	200
	300	600
	300	—
	600	—
NGC 6229	136	200
	200	600
	600	800
	800	—
	800	—
NGC 7006	600	100
	—	600
	800[a]	—
	800[a]	—
	800[a]	—

[a] Nonphotometric night.

 0004-6256/85/112254-21$00.90

TABLE II. Field centers.

Name	(1,1) Relative to cluster center (pixels)	Cursor (pixels)	g (mag)
NGC 5466			
Field 1	− 180, − 600	208,46	20.60
Field 2	− 180, − 250	—	—
Field 3	300, − 450	92,68	20.27
Field 4	300, 250	109,47	20.16
Field 5	100, 400	88,70	20.17
Field 6	− 100, 500	115,73	19.32
NGC 6229			
Field 1	− 120, − 500	150,191	20.82
Field 3	− 320, − 500	54,115	21.73
Field 4	− 130, 580	83,163	21.56
Field 5	100, 580	30,152	20.89
Field 6	150, − 500	22,158	21.50
NGC 7006			
Field 1	110, 260	130,50	20.12
Field 2	120, − 570	77,8	21.77
Field 3	− 470, 260	89,28	21.82

determined from well-isolated stars was 0.08 mag, which presumably arises from the statistics of the placement of the center of the image with respect to the center of a pixel.

The point-source detections in each of the frames of a given field were merged by a computer program, which also took into account the small shifts between frames. When there was more than one frame of a field in any given color, the magnitudes were averaged and the dispersions about the means calculated. The only manual intervention in the whole procedure was the elimination of small resolved galaxies (a maximum of three per region), and the selection of well-isolated stars and subsequent calculation of the offsets between the box magnitudes and true large-aperture magnitudes.

A discussion of the difference between the CCD/PFUEI instrumental system and the photoelectric photometry that defines the magnitudes and colors of the Thuan-Gunn system is given in Schneider, Gunn, and Hoessel (1983). However, the 4-shooter has significantly better blue response than does the PFUEI (although they both use the same 800 × 800 Texas Instruments CCD chips as detectors). Thus the transformation between our instrumental and the photoelectric $g - r$ colors has a slope significantly closer to 1.0 than was found by Schneider *et al.* This transformation was calculated from two photometric nights during each of which six bright Thuan-Gunn photometric standards were observed. The standards span the range of $g - r$ color from − 0.79 to 0.57 mag. The final averaged g and r magnitudes are listed in Tables III–V.*,† As one can see from looking at the magnitude dispersions, which are listed in the tables in units of 0.01 mag, except in those cases where the matchup between detected point sources in different frames failed (presumably due to crowding), the dispersions are quite reasonable. At these faint magnitudes, the crowding and the uncertainties in flattening of the sky dominate the errors.

b) Transformation to B,V

The transformation from g,r, to B,V was made using the bright standards of the Thuan-Gunn system with B,V magnitudes in Blanco *et al.* (1968). The standards were fit with the relationships

$$V = g - 0.371(g - r) - 0.038$$

and

$$B - V = 0.454 + 0.963(g - r)\,.$$

The dispersion of the difference between the predicted and published V and $B - V$ magnitudes was 0.02 mag, with the largest absolute value of a difference being 0.04 mag. These transformations have been used throughout this paper.

As a check of these transformations, a field in the periphery of M3 with a faint sequence by Sandage (1970) was observed in March 1985. The B,V magnitudes were calculated from the g,r magnitudes and compared with those of Sandage. For 12 stars with $16 \leqslant V \leqslant 21$ mag, the mean difference in V was 0.01 mag with a dispersion of 0.09 mag, while the mean difference in $B - V$ was 0.085 mag with a dispersion of 0.10 mag. The five photoelectric standards from Sandage and Wildey's (1967) study of NGC 7006 that were faint enough to be unsaturated in our shortest g and r frames were also used to check the transformation of photometric systems. A mean difference between V (predicted) and V (Sandage-Wildey) of 0.05 mag with a dispersion of 0.10 mag and a mean $B - V$ difference of 0.06 mag with a dispersion of 0.04 mag was found.

We note that our g magnitudes for the faintest of Baade's (1945) standards in NGC 6229 have a mean $(m_{pg} - g)$ of 0.01 mag with a dispersion about the mean of 0.24 mag. (Standard r of Baade appears to be misidentified on his plate II and we ignore it.)

III. CLUSTER AGES

a) Isochrone Fits

Figures 4–8 show the g,r, color-magnitude diagrams for the three distant halo clusters. No effort has been made to remove the known RR Lyrae variables from any of the figures. All point sources measured on at least two of the g frames and one of the r frames of NGC 5466 in fields 1 to 6 (excluding field 2, which is too crowded for reliable photometry) that are brighter than $r = 22.0$ are plotted in Fig. 4. For NGC 6229, all points in the five outlying fields studied with $r \leqslant 23.50$ mag that were measured on at least three of the g frames and two of the r frames are shown in Fig. 5. The solid line represents the mean locus of the brighter subgiants picked up in a search of an area on the frames closer to the center of NGC 6229, where crowding limits the photometry to the brightest stars only; the color-magnitude diagram for these stars is shown in Fig. 6. Figure 7 shows the stars detected on at least one of the g and r frames taken on photometric nights in fields close to the center of the cluster NGC 7006, where faint photometry is impossible because of crowding. Even at the magnitude levels shown, crowding has limited the accuracy of the magnitudes to ± 0.10 mag. Stars detected on at least two of the g frames and one of the r frames that are brighter than $r = 23.50$ mag in three small fields on the

* The five fields of NGC 6229 gave color-magnitude diagrams slightly offset from each other. These fields occurred on different chips of the 4-Shooter (as was the case for all three clusters) and each field was not always on the same chip in all the frames. The origin of this problem is unknown, but to eliminate it small offsets were made in all the g magnitudes for a given field in NGC 6229 only. The offsets did not exceed 0.05 mag, and the average of the offsets for the five fields was set equal to zero.

† Seven stars were omitted from the end of Table III to avoid having an extra page in the table with only two lines of data.

TABLE III. Magnitudes of NGC 5466 stars.

x (pix)	y	r	g-r	#	σ(r) (mag)	#	σ(g) (mag)	x (pix)	y	r	g-r	#	σ(r) (mag)	#	σ(g) (mag)	x (pix)	y	r	g-r	#	σ(r) (mag)	#	σ(g) (mag)
Field 1								153	1	21.93	0.65	1	0	2	1	232	1	19.73	0.04	1	0	3	1
265	1	20.52	0.20	1	0	3	0	77	12	20.97	0.08	2	4	4	9	120	13	21.55	0.28	2	0	3	17
239	16	21.04	1.14	2	0	3	9	140	26	21.47	0.04	2	3	3	11	226	29	20.86	0.05	2	0	4	2
10	31	21.84	-0.44	2	53	3	3	88	31	19.37	0.17	2	0	4	4	75	36	21.44	0.16	2	7	3	8
198	37	21.21	1.10	2	2	3	21	220	41	19.88	0.07	2	2	4	4	111	46	21.76	0.35	2	1	3	10
208	46	20.53	0.07	2	4	4	3	260	52	21.85	0.32	2	2	3	13	156	53	21.00	0.12	2	0	3	8
9	64	19.65	0.05	2	1	4	2	252	64	21.73	0.28	2	10	3	18	168	66	20.50	0.03	2	2	4	3
241	73	21.64	0.18	2	12	3	9	131	77	19.35	0.15	2	1	4	2	67	78	21.27	0.06	2	0	3	6
289	78	21.43	0.73	2	8	3	9	153	81	20.59	0.01	2	1	4	2	77	84	21.68	0.14	2	2	3	5
8	89	20.49	0.00	2	1	4	2	171	90	19.76	0.48	2	2	4	1	247	92	21.25	0.09	2	9	3	6
189	93	21.35	0.13	2	4	3	5	111	96	21.13	0.05	2	1	3	3	151	102	17.64	0.23	1	0	3	0
285	102	21.76	0.19	2	8	3	8	196	106	20.60	-0.02	2	5	4	2	275	106	19.58	0.04	2	5	3	2
8	108	20.57	0.00	2	3	3	3	108	111	21.92	0.15	2	3	2	2	140	113	21.31	0.00	2	6	2	0
256	113	21.06	0.15	2	5	2	11	9	116	20.70	-0.01	2	2	3	3	72	116	20.40	0.03	2	2	3	3
87	116	19.77	-0.21	2	1	3	3	240	117	21.71	0.26	2	2	2	14	115	120	21.39	0.06	2	0	3	8
133	120	21.13	0.04	2	1	3	1	202	124	21.37	0.22	2	1	3	7	215	124	20.39	0.03	2	2	4	0
235	124	21.44	0.18	2	2	3	4	12	125	21.22	0.08	2	4	3	5	147	125	21.22	0.14	2	3	3	1
58	126	21.65	0.09	2	2	3	3	25	127	18.57	0.24	1	0	4	2	270	127	20.79	0.07	2	3	4	6
218	133	21.29	0.16	2	1	3	2	26	137	21.78	0.17	1	0	2	3	192	140	20.82	0.03	2	2	4	5
218	144	20.00	-0.01	2	3	4	1	12	147	21.75	0.09	2	3	3	8	123	147	20.74	0.00	2	0	4	5
30	148	21.93	-0.05	2	14	2	18	55	148	21.03	-0.09	2	5	3	5	256	148	20.39	0.05	2	3	4	4
219	149	20.90	0.04	2	1	2	0	150	155	20.73	0.10	2	0	4	5	188	155	21.56	0.34	2	3	3	4
209	155	20.98	0.08	2	0	3	3	273	157	19.53	0.05	2	6	4	2	284	157	21.18	0.19	2	4	3	4
145	160	20.77	0.04	2	3	4	7	217	161	21.06	0.09	2	3	3	1	248	165	20.71	0.07	2	1	4	0
224	168	20.95	0.02	2	2	3	1	58	171	21.73	0.08	2	1	3	6	157	172	21.79	0.03	2	0	3	10
12	173	18.55	0.28	1	0	4	2	269	173	19.82	0.04	2	5	4	1	87	175	20.82	0.01	2	1	3	2
41	179	20.88	0.01	2	2	3	2	158	179	20.78	-0.02	2	1	3	5	261	180	21.77	0.16	2	1	3	1
105	181	20.03	0.03	2	1	4	6	222	183	21.76	0.16	2	0	3	7	293	183	20.49	0.08	1	0	4	2
30	185	21.59	0.10	2	3	3	8	67	186	21.71	0.14	2	8	3	5	120	186	20.92	-0.12	2	12	3	14
96	187	21.68	0.02	2	0	3	6	254	189	21.75	0.32	2	2	3	5	56	190	21.19	0.00	2	3	3	5
229	191	21.63	0.10	2	4	3	0	40	192	20.71	-0.04	2	4	4	4	183	192	19.89	0.00	2	0	4	3
35	197	19.96	0.00	2	3	4	4	257	198	21.44	0.21	2	0	3	9	7	199	20.60	-0.01	2	2	4	5
183	202	21.69	0.13	2	2	3	4	18	203	20.93	0.01	2	4	3	2	287	204	21.26	0.14	2	2	3	2
294	204	21.96	0.22	1	0	3	1	6	206	20.15	0.01	2	2	4	4	140	206	21.87	0.22	2	8	3	18
195	207	21.36	0.09	2	1	2	13	181	208	20.33	0.03	2	2	4	7	52	213	21.85	0.06	2	3	3	9
43	214	19.35	0.03	2	2	4	3	74	216	21.85	0.20	2	3	3	4	169	218	21.80	0.03	2	0	3	11
277	221	21.52	0.64	2	39	2	24	257	222	19.75	0.05	2	0	4	1	32	224	21.94	0.08	2	2	3	9
122	225	20.95	-0.01	2	14	3	5	292	225	21.82	0.43	1	0	3	2	223	227	20.18	0.04	2	5	4	7
244	227	21.81	0.25	2	0	3	6	280	230	17.36	1.29	1	0	4	2	168	231	21.86	0.06	2	15	3	19
51	232	20.63	0.07	2	2	4	5	16	234	20.92	0.04	2	0	3	3	156	234	20.44	0.04	2	5	4	9
92	235	21.64	0.10	2	0	3	8	230	235	19.40	0.13	2	1	4	5	58	236	21.23	0.01	2	2	3	4
187	236	20.32	0.05	2	0	4	6	74	237	20.77	0.09	2	0	4	6	86	237	21.71	0.10	2	1	3	9
150	237	21.41	-0.01	2	22	3	19	174	237	19.93	0.02	2	0	4	5	203	237	21.27	0.13	2	2	3	5
292	239	20.85	0.12	1	0	3	1	234	240	20.12	-0.04	2	0	4	6	96	242	21.08	-0.30	2	36	3	2
135	242	20.81	0.12	1	0	3	18	223	242	21.87	0.08	2	10	3	13	199	244	21.33	0.06	2	1	3	9
232	244	19.86	0.05	2	0	4	8	59	246	21.50	0.06	2	2	3	8	93	246	21.33	0.12	2	3	3	5
101	246	21.72	-0.06	1	0	3	9	23	248	17.39	0.30	1	0	3	2	141	250	21.51	0.04	2	2	3	15
110	251	21.19	0.09	2	2	3	8	180	252	19.90	0.03	2	1	4	5	131	253	21.52	0.07	2	5	3	11
121	255	21.59	0.20	2	3	3	7	189	257	21.35	0.05	2	1	3	5	66	258	19.11	0.19	2	2	4	4

TABLE III. (continued)

x (pix)	y	r	g-r	#	$\sigma(r)$ (mag)	#	$\sigma(g)$ (mag)	x (pix)	y	r	g-r	#	$\sigma(r)$ (mag)	#	$\sigma(g)$ (mag)	x (pix)	y	r	g-r	#	$\sigma(r)$ (mag)	#	$\sigma(g)$ (mag)
255	258	20.80	0.08	2	1	4	7	223	259	19.94	0.02	2	1	4	4	202	260	21.84	0.16	2	0	3	6
275	260	21.29	0.14	2	4	3	4	154	261	21.56	0.19	2	1	3	11	162	261	21.40	0.06	2	2	3	9
115	262	20.88	0.01	2	1	3	4	295	263	19.50	0.26	1	0	3	4	130	264	20.84	0.02	2	2	3	6
90	265	21.06	0.06	2	2	2	3	12	272	21.17	0.12	2	0	3	1	273	272	21.20	0.10	2	2	3	3
213	273	20.47	-0.01	2	1	4	6	102	276	19.48	0.14	2	1	4	5	50	279	20.22	0.03	2	1	4	1
130	279	20.97	0.02	2	1	3	6	214	281	20.65	0.15	2	2	4	14	255	282	19.52	0.07	2	2	4	7
287	282	20.04	0.08	2	2	4	8	193	284	21.07	0.06	2	5	3	10	76	286	20.80	0.08	2	3	3	2
292	286	20.96	0.12	1	0	3	2	141	287	21.41	0.08	2	0	3	7	24	288	21.51	0.19	2	2	3	5
50	289	21.56	0.14	2	5	3	13	38	292	21.59	0.08	2	7	3	10	7	294	20.18	0.04	2	2	3	3
56	295	19.32	0.12	2	2	3	4	236	296	21.77	0.21	1	0	2	5	20	297	20.94	-0.05	1	0	2	1
190	297	20.59	-0.09	2	4	2	0																
Field 3								54	11	20.78	0.04	2	0	4	9	100	20	21.86	0.40	2	3	3	22
93	21	19.99	0.00	2	2	4	3	58	26	19.90	0.01	2	2	4	2	121	26	20.61	0.07	2	1	4	3
23	27	21.36	0.09	2	1	3	6	12	31	21.38	0.19	2	2	3	9	53	31	20.45	-0.01	2	1	4	6
71	31	20.83	0.09	2	5	4	8	125	33	20.49	0.07	2	2	4	4	110	40	21.31	0.22	2	4	3	12
120	40	21.21	0.15	2	1	3	10	72	55	20.31	0.02	2	4	4	6	39	58	21.93	0.35	2	3	3	18
11	59	20.98	0.14	1	0	4	10	16	60	21.09	0.14	2	7	3	19	111	61	21.66	0.73	1	0	2	1
45	64	20.56	0.65	2	2	3	8	104	65	20.63	0.07	2	3	4	8	92	68	20.21	0.06	2	3	4	6
9	77	20.31	-0.02	2	5	4	3	47	77	20.38	1.07	2	3	3	13	58	82	20.51	0.08	2	4	4	5
128	87	20.80	0.07	2	4	4	5	107	90	21.11	0.15	2	5	3	7	88	91	21.82	0.52	2	8	3	18
128	95	21.80	0.29	2	7	3	20	133	97	21.33	0.13	1	0	3	10	18	98	19.92	0.04	2	4	4	7
81	100	21.59	0.49	2	5	3	16	34	101	20.34	0.05	2	2	4	3	54	102	19.97	-0.01	2	0	4	3
109	103	21.90	0.19	2	12	3	12	105	109	21.73	0.15	2	6	3	6	34	122	18.60	0.18	1	0	4	2
72	122	19.77	0.04	2	0	4	2	106	125	21.48	0.23	2	8	3	3	5	133	20.31	0.12	1	0	2	3
99	134	21.29	0.15	2	0	3	4	26	137	21.57	-0.05	2	25	3	11	39	140	20.01	0.00	2	1	4	2
53	142	21.83	0.30	2	0	3	8	105	145	18.77	0.22	1	0	4	1	77	148	19.70	0.05	2	0	4	1
10	150	21.75	0.18	1	0	3	20	57	151	20.54	0.09	2	0	4	9	75	156	20.69	0.04	2	1	4	3
67	158	21.10	0.07	2	1	3	2	137	163	21.80	0.20	1	0	2	0	92	175	20.99	0.01	2	2	3	1
49	176	19.52	0.06	2	1	3	4	113	179	21.45	0.06	2	2	3	0	120	185	18.22	0.26	1	0	4	2
56	191	20.34	0.04	2	0	4	10	21	192	20.53	0.07	2	2	4	8	9	195	21.58	0.27	1	0	3	9
42	199	21.06	-2.20	2	4	2	0	17	200	20.93	0.09	2	4	3	1	59	202	20.16	-0.01	2	2	4	4
38	203	19.17	0.26	2	1	2	5	129	203	21.07	-0.03	2	4	3	8	105	207	21.97	0.13	2	1	3	4
129	212	20.47	0.02	2	2	4	9	23	215	20.59	-0.01	2	3	3	5	124	218	21.08	-0.03	2	2	3	7
67	219	21.86	-0.20	2	19	3	1	12	225	21.52	0.13	2	0	3	3	42	227	21.16	0.26	2	10	3	4
69	228	21.41	0.13	2	5	3	6	50	229	20.21	0.03	2	1	4	9	112	231	21.67	0.19	2	6	3	24
133	233	20.04	0.09	1	0	4	3	53	235	21.35	-0.01	2	3	3	7	94	242	19.83	0.02	2	2	4	3
70	244	21.28	0.07	2	2	3	9	106	248	21.51	-0.03	2	3	3	15	37	250	21.63	0.26	2	7	3	8
52	250	21.99	0.26	2	3	3	3	18	253	20.37	0.03	2	3	4	5	97	255	20.70	0.03	2	5	4	12
41	256	21.55	0.28	2	6	3	2	76	258	21.15	0.08	2	1	3	4	84	258	20.69	-0.01	2	3	4	4
50	260	20.40	0.06	2	3	4	2	69	260	21.34	-0.01	2	1	3	4	107	261	20.57	0.04	2	2	4	4
38	262	21.39	0.08	2	0	3	3	32	266	21.11	0.09	2	3	3	2	69	267	19.55	0.01	2	0	4	1
79	268	21.21	0.13	2	3	3	1	22	270	21.31	0.15	2	1	3	4	122	270	21.20	-0.09	2	3	3	6
52	271	20.30	0.05	2	1	4	2	5	273	20.00	0.03	2	1	2	0	104	274	21.95	0.15	2	2	3	6
70	276	21.59	0.06	2	4	3	2	110	276	21.66	0.13	2	4	3	5	49	277	20.43	-0.02	2	2	4	3
59	280	20.60	0.00	2	1	4	3	100	282	20.63	0.01	2	3	4	1	10	284	21.20	0.19	2	0	3	7
65	288	21.46	0.37	1	0	3	11	76	291	21.97	0.46	2	2	3	12	113	291	19.07	0.13	2	1	4	3
19	292	19.94	0.05	2	0	4	4	64	295	20.92	-0.01	2	1	3	5	90	295	21.77	0.12	2	8	3	0
56	296	21.11	0.13	2	1	3	0	42	300	21.77	0.30	2	2	3	14	77	301	20.87	0.02	2	1	3	0
75	307	20.48	0.02	2	1	4	1	23	308	20.80	0.21	2	2	3	2	138	312	21.39	0.10	1	0	2	0

TABLE III. (continued)

x (pix)	y	r	g-r	#	$\sigma(r)$ (mag)	#	$\sigma(g)$ (mag)	x (pix)	y	r	g-r	#	$\sigma(r)$ (mag)	#	$\sigma(g)$ (mag)	x (pix)	y	r	g-r	#	$\sigma(r)$ (mag)	#	$\sigma(g)$ (mag)
49	314	20.55	0.02	2	1	4	10	106	318	21.17	0.13	2	2	3	2	75	320	21.60	-0.37	2	48	3	3
118	321	21.87	0.12	2	0	3	7	13	322	20.32	0.10	2	2	4	5	119	329	21.09	0.17	2	1	3	6
123	330	21.18	0.10	2	4	3	7	92	333	21.40	0.19	2	1	3	6	9	334	20.85	0.25	2	1	3	7
85	334	21.37	0.43	2	13	3	15	54	335	21.91	0.07	2	1	3	16	127	335	20.30	-0.05	2	1	4	4
94	339	21.50	0.23	2	2	3	3	26	340	19.97	0.02	2	2	4	6	75	340	21.28	0.21	2	1	3	10
37	341	21.29	0.26	2	4	3	21	15	343	20.16	0.07	2	1	4	5	6	346	20.34	-0.02	2	0	2	3
121	346	21.85	0.27	2	4	3	4	64	347	20.18	0.03	2	0	4	1	88	350	21.46	0.03	1	0	2	1
10	352	19.57	0.08	2	0	4	8	96	352	19.94	0.02	2	0	4	3	20	353	20.10	-0.04	2	1	4	1
85	355	20.08	0.01	2	1	4	4	59	356	19.44	-0.02	2	2	4	2	68	357	18.93	0.18	2	0	4	2
20	358	19.82	0.01	2	0	4	4	122	360	21.81	0.29	2	3	3	6	53	365	21.05	0.16	2	5	3	11
11	366	20.14	0.06	2	0	4	5	103	366	20.33	0.09	2	2	4	6	31	367	20.65	0.08	2	3	4	7
41	368	21.36	0.22	2	1	3	10	20	369	19.66	0.00	2	2	4	8	66	370	21.62	0.35	2	6	3	8
91	370	20.94	0.12	2	3	3	4	124	370	22.00	0.15	2	10	3	4	131	370	21.23	0.17	1	0	3	2
48	372	20.50	0.13	2	0	4	5	30	373	21.60	0.44	2	5	3	14	108	373	21.13	0.14	2	8	3	4
39	375	21.66	0.30	2	7	3	6	84	376	19.54	0.03	2	1	4	4	115	377	20.48	0.02	2	0	4	1
71	378	20.09	0.10	2	1	4	5	13	380	19.89	0.01	2	1	4	4	59	380	21.03	0.18	2	7	3	11
124	380	20.02	0.01	2	1	4	4	34	382	20.24	0.05	2	1	4	4	67	385	21.25	0.13	2	10	2	0
9	388	21.57	0.30	2	11	2	0	97	388	18.45	0.20	1	0	3	3	16	389	20.49	0.05	2	2	3	4
73	389	20.53	0.10	2	4	3	6	38	391	20.18	0.06	2	1	3	5	76	394	21.60	0.52	1	0	2	1
95	394	20.29	0.04	2	3	3	3	122	395	21.07	0.10	2	6	3	2								
Field 4								23	4	20.02	0.01	1	0	2	1	14	5	20.79	0.12	1	0	2	2
116	5	20.02	0.04	2	3	4	1	45	6	18.93	0.19	2	2	4	2	88	6	21.30	0.22	2	7	3	4
107	6	21.80	0.02	2	10	3	8	62	7	20.81	0.04	2	6	4	5	73	7	19.71	0.03	2	3	4	4
131	8	20.56	0.09	2	6	4	3	26	9	19.81	0.04	2	2	4	2	92	11	21.18	0.18	2	8	3	5
9	14	19.75	-0.05	2	2	4	4	19	18	19.86	0.01	2	2	4	3	58	18	21.13	0.13	2	7	3	4
79	18	19.06	0.46	2	1	4	49	127	20	21.04	0.09	2	4	3	2	5	21	21.12	0.04	2	4	3	12
75	23	20.24	-0.02	2	1	3	1	45	24	21.54	0.16	2	11	3	2	66	24	19.96	0.07	2	2	4	3
89	26	21.84	0.24	2	5	3	1	115	26	19.21	0.07	2	2	4	4	53	28	21.89	0.31	2	18	3	7
21	29	21.95	0.27	2	15	2	2	135	30	21.77	0.20	2	17	3	15	77	31	21.14	-0.80	2	4	2	2
121	33	21.30	0.09	2	7	3	2	128	33	21.84	0.25	2	15	2	19	10	34	20.69	-0.01	2	6	4	4
39	34	20.21	-0.03	2	4	4	3	87	34	20.62	0.05	2	3	4	0	49	35	20.95	0.12	2	7	4	4
76	35	20.39	0.03	2	3	2	2	107	35	19.01	-0.28	2	2	4	4	126	36	21.90	0.30	1	0	2	20
4	37	19.68	0.02	2	2	4	4	65	38	19.45	0.07	2	1	4	2	53	39	20.21	0.06	2	4	4	3
64	44	20.27	0.27	2	2	4	34	124	44	20.50	0.07	2	5	4	1	59	47	20.91	0.13	2	4	2	11
109	47	20.15	0.01	2	4	4	1	10	51	21.33	0.20	2	7	3	11	116	56	21.86	0.29	2	8	3	14
88	57	21.83	0.46	2	14	3	17	106	57	20.82	0.21	2	5	4	20	133	57	21.08	0.27	2	8	3	23
10	58	21.96	-0.80	2	16	3	58	66	58	21.97	0.10	1	0	2	9	96	60	20.77	0.08	2	3	4	8
122	61	21.73	0.18	2	15	3	9	129	61	21.49	0.14	2	10	2	14	24	62	21.73	0.38	2	10	3	12
7	64	20.74	-0.29	2	31	3	4	12	64	21.22	0.13	1	0	2	9	58	64	19.92	0.00	2	4	4	5
36	65	19.88	0.02	2	4	4	2	64	67	19.73	0.00	2	1	4	1	86	67	21.76	0.26	2	2	3	21
48	69	20.00	-0.02	2	3	4	2	132	70	21.64	0.16	2	12	3	6	84	72	21.51	0.22	2	8	2	4
117	73	20.94	0.13	2	4	3	4	106	76	18.23	0.21	1	0	4	1	62	77	20.97	0.10	2	4	3	3
27	79	17.48	0.24	1	0	3	3	25	87	19.98	-0.06	2	3	4	6	126	88	21.54	0.04	1	0	3	2
107	90	21.00	0.13	2	8	3	4	72	91	20.68	0.19	1	0	4	2	40	92	21.17	0.05	2	3	3	1
52	92	20.10	0.00	2	2	4	1	64	94	20.89	0.15	2	1	3	13	36	97	21.04	0.17	2	0	2	2
22	99	20.56	-0.02	2	2	4	3	48	99	21.77	0.31	1	0	3	7	56	101	20.25	-0.27	2	26	4	4
97	101	21.77	0.07	2	20	3	5	123	102	19.99	0.01	2	1	4	1	103	103	20.60	0.07	2	3	4	2
79	104	20.03	0.04	2	1	4	2	21	106	18.39	0.22	1	0	4	2	48	106	20.94	0.08	2	4	3	3
29	108	20.34	-0.08	2	1	4	1	40	110	20.12	0.05	2	1	4	1	100	111	21.99	0.19	2	11	3	9

TABLE III. (continued)

x (pix)	y	r	g-r	#	$\sigma(r)$ (mag)	#	$\sigma(g)$ (mag)	x (pix)	y	r	g-r	#	$\sigma(r)$ (mag)	#	$\sigma(g)$ (mag)	x (pix)	y	r	g-r	#	$\sigma(r)$ (mag)	#	$\sigma(g)$ (mag)
4	112	20.67	0.08	2	4	2	2	33	114	21.22	0.10	2	5	2	1	49	119	20.08	0.02	2	1	4	1
22	121	20.70	0.05	2	0	4	2	14	123	18.37	-0.09	1	0	4	2	34	124	20.07	-0.01	2	0	4	1
55	127	19.24	-1.08	2	122	3	1	89	127	21.58	0.27	2	6	2	0	127	127	19.52	-0.03	2	3	4	2
23	131	19.55	0.02	2	1	4	1	132	132	21.10	0.04	2	6	3	1	35	133	20.72	0.04	2	0	4	1
6	134	20.36	0.04	2	1	4	1	84	136	21.10	0.06	2	7	3	4	113	136	20.67	0.03	2	2	3	4
39	137	20.72	0.02	2	5	4	2	54	137	19.86	0.50	2	1	4	79	13	140	20.78	0.03	2	3	4	3
49	142	21.42	0.38	2	2	3	13	89	142	20.29	-0.43	2	2	3	44	114	142	19.86	-0.12	2	1	4	3
84	145	19.46	-0.24	2	1	3	1	24	146	20.89	0.25	2	3	3	2	61	148	18.33	0.23	1	0	4	1
96	156	21.75	0.27	2	9	3	12	38	158	21.35	0.14	2	0	3	9	60	158	20.71	0.05	2	3	4	2
108	158	19.23	0.12	2	2	4	1	23	159	19.95	0.04	2	1	4	2	122	159	21.24	0.27	2	7	3	6
39	164	21.48	0.12	2	7	2	1	73	166	21.22	0.14	2	5	3	4	91	166	21.14	0.10	2	6	3	4
34	167	21.37	0.25	2	6	3	5	107	167	20.42	0.02	2	3	4	3	97	177	19.82	0.01	2	2	4	3
42	178	19.19	-0.27	2	1	4	1	48	178	19.84	-0.05	2	0	4	2	11	183	19.34	0.08	2	1	4	1
110	184	20.13	0.01	2	1	4	2	63	186	21.26	0.15	2	1	3	6	20	187	20.75	0.15	2	1	4	3
31	189	20.75	0.13	2	3	3	1	51	189	21.76	0.20	2	3	3	7	134	189	21.52	0.14	1	0	3	7
88	194	20.51	0.06	2	1	4	4	118	194	19.27	0.10	2	1	4	1	128	195	21.27	0.07	2	4	3	1
50	197	21.02	0.07	2	0	3	3	10	198	21.58	0.22	2	3	3	9	101	200	21.76	0.26	2	6	3	8
115	201	20.96	-0.01	2	4	4	4	1	202	20.04	0.02	1	0	3	0	40	204	21.38	0.37	2	3	3	34
36	207	21.71	-0.19	2	16	2	5	12	208	21.48	0.10	2	5	3	3	25	212	21.76	0.23	2	10	3	8
52	214	20.92	0.80	2	1	3	54	106	214	21.21	0.15	2	3	3	4	131	215	20.23	0.03	2	0	4	1
42	220	20.50	0.03	2	4	4	1	89	221	21.82	0.01	2	8	3	18	129	224	20.87	0.23	2	0	3	2
85	225	21.51	0.20	2	4	2	13	18	226	19.35	0.10	2	2	4	2	29	227	20.22	0.02	2	0	4	1
2	237	20.82	0.06	2	0	3	4	32	240	19.82	0.01	2	0	4	0	133	241	19.87	0.02	2	1	4	1
75	242	20.83	0.05	2	1	4	1	23	243	21.15	0.12	2	0	3	3	66	243	20.56	0.10	2	1	4	4
54	244	20.65	0.04	2	1	4	2	87	245	20.10	0.02	2	1	4	1	93	245	20.90	-0.04	2	0	3	1
115	245	18.20	0.21	1	0	4	2	104	246	20.00	0.02	2	1	4	1	46	248	21.30	0.16	2	4	3	4
15	249	20.83	0.00	2	0	4	2	10	250	21.03	0.04	2	1	3	3	48	255	21.28	0.22	2	2	3	6
124	256	20.88	0.13	2	3	3	4	71	261	20.62	0.15	2	1	4	4	82	261	20.28	-0.01	2	4	4	4
10	263	21.04	0.14	2	6	3	4	110	263	20.63	0.05	2	2	4	1	0	266	19.66	-0.17	2	7	3	5
36	269	21.49	0.14	2	3	3	3	107	271	19.47	-0.01	2	2	4	4	41	273	21.83	0.20	2	3	3	9
33	275	21.97	0.46	2	0	3	11	119	278	20.65	0.07	2	2	4	1	7	280	20.98	0.06	2	1	3	2
81	283	21.85	0.18	2	4	3	10	67	284	20.10	0.05	2	1	4	6	117	285	21.81	0.19	2	4	3	2
48	288	21.17	0.26	2	4	2	5	18	292	19.77	0.01	2	3	4	2	53	292	20.58	0.08	2	1	4	2
56	299	20.66	0.06	2	2	4	5	86	300	21.56	0.14	2	1	3	2	21	301	21.70	0.24	2	0	3	1
6	306	21.80	0.13	1	0	3	2	18	308	20.68	0.02	1	0	4	6	125	310	20.93	0.12	2	2	3	1
40	311	22.00	0.45	2	3	3	9	13	314	21.36	0.03	2	11	3	4	79	314	21.13	0.09	2	1	3	0
31	323	20.45	0.00	2	3	4	2	102	334	21.20	0.05	2	1	3	2	40	335	21.55	0.23	2	1	2	0
88	336	18.06	0.28	1	0	4	2	58	338	19.64	0.00	2	5	4	3	106	339	20.98	0.17	2	3	3	0
37	350	21.51	0.14	2	4	3	1	85	350	19.89	0.04	2	3	4	5	133	351	18.32	0.41	1	0	4	25
54	354	20.18	0.04	2	4	4	2	21	361	21.72	0.14	2	3	2	0	14	365	19.68	-0.01	1	0	4	4
28	365	21.05	0.04	2	3	3	5	43	367	19.56	0.06	2	5	4	5	116	367	20.73	0.01	2	1	4	3
112	373	21.62	0.27	1	0	3	13	83	378	20.81	0.04	2	4	3	3	23	382	17.79	0.31	1	0	4	5
111	384	20.44	0.04	2	3	3	1																
Field 5								2	2	19.19	-0.04	1	0	3	5	72	3	21.17	0.02	2	2	2	5
112	5	20.40	0.02	2	1	4	5	96	6	20.46	0.03	2	3	4	4	90	8	21.37	0.05	2	1	3	7
77	9	19.42	-0.19	2	2	4	3	5	13	20.39	-0.02	2	3	4	7	23	13	20.89	-0.04	2	6	3	12
93	14	21.09	0.02	2	2	3	5	50	16	20.34	-0.02	2	8	4	4	38	17	19.90	-0.03	2	21	4	22
87	17	21.83	-0.02	2	1	3	7	79	18	20.40	-0.03	2	0	4	2	18	19	19.14	0.12	2	3	4	3
98	19	21.22	0.06	2	1	3	9	61	21	20.64	0.05	2	3	4	7	8	22	20.10	-0.02	2	6	4	7

TABLE III. (continued)

x (pix)	y	r	g-r	#	$\sigma(r)$ (mag)	#	$\sigma(g)$ (mag)	x (pix)	y	r	g-r	#	$\sigma(r)$ (mag)	#	$\sigma(g)$ (mag)	x (pix)	y	r	g-r	#	$\sigma(r)$ (mag)	#	$\sigma(g)$ (mag)
109	23	20.92	-0.01	2	5	3	3	76	24	20.49	0.02	2	0	4	7	91	24	20.06	-0.01	2	2	4	5
102	26	19.50	0.03	2	1	4	5	61	29	19.18	0.10	2	3	4	4	23	32	20.81	-0.10	2	29	3	24
12	33	19.54	-0.15	2	45	4	35	101	33	19.50	0.01	2	1	4	3	43	35	21.03	0.10	2	3	3	6
82	35	20.39	-0.02	2	4	4	9	108	35	20.50	0.02	2	3	4	8	25	36	20.60	0.06	1	0	2	4
34	38	21.33	0.10	2	0	3	0	81	40	20.27	0.00	2	2	2	3	96	41	20.92	0.02	2	6	3	3
114	42	16.87	0.28	1	0	3	3	24	43	20.32	0.02	2	0	4	5	12	46	20.23	0.00	2	3	4	6
3	48	20.68	0.08	1	0	3	6	82	49	19.18	0.03	2	3	4	3	54	50	21.32	-0.26	2	1	3	38
91	52	21.15	-0.01	2	1	2	0	109	53	19.99	0.25	2	7	4	7	39	55	20.11	-0.01	2	2	4	5
53	55	20.62	-0.08	2	18	4	16	48	56	20.82	-0.06	1	0	2	4	83	57	19.92	-0.09	2	1	4	4
10	58	20.41	0.01	2	1	4	10	72	58	21.77	0.18	1	0	3	12	65	59	21.74	0.25	2	4	3	2
16	62	20.65	0.03	2	2	4	10	28	63	21.89	0.17	2	6	3	7	4	64	20.97	-0.03	2	1	3	4
104	65	19.38	-0.21	2	1	4	5	113	65	20.40	-0.01	2	4	3	5	10	68	21.39	0.18	2	7	3	7
70	68	21.70	0.21	2	2	3	5	55	70	20.62	0.18	2	2	4	4	63	70	21.10	0.09	2	2	3	3
88	70	20.18	-0.01	2	2	4	5	18	71	21.36	0.17	2	3	2	0	36	72	20.00	0.05	2	2	4	2
47	74	19.86	0.00	2	2	4	3	113	74	19.31	0.07	2	2	4	4	5	76	20.39	-0.03	2	3	3	5
27	81	21.58	0.00	1	0	2	4	51	82	20.68	0.09	2	1	4	6	63	82	21.08	0.02	2	1	3	4
73	82	20.85	0.05	2	3	4	7	79	82	21.75	-0.10	2	3	3	6	109	83	19.45	0.05	2	1	4	5
18	85	20.92	0.05	2	6	3	6	36	85	20.16	0.01	2	0	4	3	26	87	20.97	0.03	2	7	2	9
50	89	20.22	0.07	2	2	4	9	64	89	21.64	0.07	2	3	3	3	103	90	21.78	0.03	2	0	3	6
6	91	21.22	0.04	2	4	3	5	28	93	19.93	-0.07	2	5	3	2	94	96	21.92	0.14	2	0	2	3
73	97	21.08	0.03	2	2	3	7	17	98	21.43	0.05	2	1	3	3	4	99	21.87	0.12	2	5	3	1
64	100	19.59	0.04	2	3	4	4	103	103	21.47	0.02	1	0	3	4	72	106	21.68	0.13	2	0	3	5
36	110	21.17	0.05	2	2	3	4	5	111	21.98	0.35	1	0	2	2	54	111	21.71	-0.20	2	10	3	3
20	115	20.99	0.00	2	2	3	4	50	115	21.81	0.10	2	4	3	3	78	115	20.90	0.04	2	1	3	2
5	116	21.57	0.76	2	2	3	7	65	120	19.33	-0.06	2	2	4	4	77	122	20.18	-0.02	2	3	4	5
9	123	21.62	0.13	2	5	3	5	0	126	21.43	0.12	1	0	2	4	35	126	20.92	-0.02	2	2	3	2
90	126	20.88	0.04	2	0	4	4	6	129	21.02	0.02	2	3	3	2	113	131	21.44	0.04	2	5	3	4
5	134	21.26	-0.02	2	2	3	3	95	135	20.64	0.00	2	0	4	7	78	140	19.65	-0.03	2	4	4	6
89	141	21.03	0.04	2	0	3	7	17	143	20.73	0.00	2	2	4	5	63	145	19.19	0.10	2	4	4	5
34	148	19.57	-0.03	2	3	4	1	87	148	21.25	0.00	2	1	3	7	82	151	21.02	0.01	2	3	3	4
37	153	19.21	1.06	2	3	4	2	73	153	21.41	0.05	2	0	3	4	-1	154	19.95	-0.05	1	0	2	1
88	157	21.39	0.02	2	0	3	3	24	159	21.89	0.22	2	3	3	6	17	167	21.76	0.01	2	0	2	0
17	174	19.87	-0.03	2	3	4	3	3	179	20.62	0.03	2	2	3	10	24	180	21.37	-0.02	2	0	3	4
48	180	19.42	0.02	2	4	4	3	57	181	21.26	-0.70	2	64	2	1	31	183	19.97	0.19	2	3	4	40
88	184	19.86	0.03	2	3	4	5	43	185	20.83	-0.03	2	2	4	7	59	185	20.72	0.10	1	0	2	8
101	185	21.87	0.08	2	0	3	5	26	188	20.70	0.07	2	9	3	1	39	188	20.49	0.00	2	4	4	5
114	188	20.07	-0.06	1	0	3	4	52	190	21.16	0.08	2	4	3	4	35	193	21.00	-0.60	2	5	3	45
52	195	21.24	0.10	2	3	2	3	4	198	20.54	0.05	1	0	3	4	39	198	20.27	-0.04	2	3	2	1
101	201	20.88	0.02	2	3	3	2	113	204	20.06	0.03	2	2	4	4	37	205	21.53	0.07	2	2	3	2
65	205	21.91	0.13	2	4	3	1	86	205	20.37	0.13	2	3	4	21	4	211	20.88	0.34	2	2	3	2
108	211	20.73	0.12	2	5	4	8	25	212	21.72	-0.03	2	4	3	8	26	217	21.52	0.12	2	2	2	3
85	217	18.04	0.22	1	0	4	1	101	217	19.24	0.12	2	2	4	4	58	218	21.16	0.02	2	2	3	1
16	226	20.99	0.07	2	1	3	6	5	227	21.67	-0.31	2	29	2	2	41	228	21.89	0.15	2	2	3	3
0	232	20.35	-0.04	1	0	2	1	61	235	21.44	0.00	2	2	3	2	11	238	21.31	0.12	2	1	3	1
65	239	21.55	0.08	2	4	3	8	81	242	20.65	-0.01	2	2	4	9	30	244	20.27	-0.01	2	1	4	4
2	246	21.23	0.13	1	0	2	2	76	246	19.71	-0.01	2	0	4	3	35	248	20.99	-0.01	2	0	4	6
53	248	20.95	-0.01	2	0	3	3	12	249	21.15	0.06	2	0	3	1	30	255	20.25	-0.06	2	0	4	1
17	262	19.89	-0.05	2	0	4	1	64	266	21.57	0.42	2	1	3	2	54	268	20.42	-0.02	2	0	4	3
110	268	21.09	-0.06	2	7	3	3	57	275	21.93	0.21	2	3	2	3	111	277	21.16	0.13	2	4	3	1

TABLE III. (continued)

x (pix)	y	r	g-r	#	$\sigma(r)$ (mag)	#	$\sigma(g)$ (mag)	x (pix)	y	r	g-r	#	$\sigma(r)$ (mag)	#	$\sigma(g)$ (mag)	x (pix)	y	r	g-r	#	$\sigma(r)$ (mag)	#	$\sigma(g)$ (mag)
97	278	20.68	0.09	2	4	4	4	32	286	21.86	0.31	1	0	3	4	54	291	20.33	-0.03	2	1	4	2
85	291	21.72	0.17	2	7	3	7	44	293	21.91	0.32	1	0	3	5	24	294	20.96	0.01	2	2	4	4
78	305	21.56	0.10	2	10	3	4	107	313	19.32	0.01	2	0	4	1	38	315	20.36	0.03	2	4	4	2
19	320	21.52	0.37	2	6	3	13	28	323	21.63	0.01	2	6	3	9	59	323	20.14	-0.02	2	5	4	3
100	332	21.92	0.23	2	7	3	10	61	334	21.29	0.12	2	4	3	6	21	345	21.59	0.04	1	0	2	3
Field 6								147	5	19.35	0.01	1	0	2	1	57	6	22.00	0.20	2	4	2	7
68	6	21.94	0.27	2	1	3	5	120	6	17.76	0.20	1	0	3	1	21	9	19.29	0.09	2	0	4	0
91	10	21.95	-0.15	1	0	3	22	81	14	20.11	0.04	2	0	4	6	111	14	19.85	0.04	2	2	4	3
27	15	21.05	0.10	2	2	3	1	88	15	21.64	0.24	2	5	2	5	17	18	21.26	0.12	2	0	3	1
118	18	20.19	0.04	2	1	4	3	142	18	20.56	0.03	2	0	4	4	54	19	20.00	0.05	2	2	4	1
42	22	19.04	-0.03	2	0	4	2	80	22	21.93	0.13	2	11	3	9	20	24	21.93	0.14	2	1	3	5
101	24	20.99	0.12	2	2	3	2	75	25	21.78	0.22	2	0	3	5	111	25	21.47	0.10	2	2	3	6
139	25	21.91	0.09	2	6	3	11	146	25	19.41	0.03	2	0	3	1	119	26	20.77	-0.01	2	4	4	2
124	28	19.35	0.06	2	0	4	3	56	34	20.01	0.01	2	0	4	2	110	34	19.71	0.00	2	1	4	1
144	36	21.64	0.20	2	9	2	7	8	38	20.60	0.05	2	4	4	3	39	38	21.60	0.22	2	3	3	0
97	38	18.99	0.17	2	0	4	1	119	38	20.64	0.02	2	2	4	3	84	39	17.32	0.25	1	0	3	1
28	40	21.61	0.19	2	3	3	3	49	47	19.56	-0.06	2	1	4	1	55	49	21.30	0.12	2	3	2	2
80	51	21.94	0.19	2	14	2	6	38	52	20.94	0.06	1	0	3	0	95	52	21.61	0.53	2	5	3	23
43	54	21.01	0.35	2	3	4	50	114	56	20.74	0.17	2	1	4	4	130	60	21.78	0.19	2	5	3	3
39	61	21.64	0.16	2	1	3	1	89	63	21.78	0.22	2	0	3	6	123	65	21.53	0.13	2	3	3	3
98	66	21.76	0.18	2	4	3	1	118	66	21.93	0.24	2	1	3	6	62	69	20.84	0.05	2	1	4	1
7	72	20.19	-0.08	2	1	4	2	115	73	19.23	0.09	2	0	4	1	140	77	21.63	0.21	2	2	3	2
101	82	21.31	0.07	2	3	3	1	75	83	21.39	0.17	2	2	3	0	143	84	21.53	0.07	2	2	3	4
95	88	20.28	0.01	2	0	4	3	101	89	21.63	0.08	2	3	2	5	141	91	21.91	0.24	2	4	2	3
81	95	20.96	0.07	2	3	3	1	103	95	21.64	0.16	2	1	3	4	43	99	21.27	0.13	2	0	3	1
133	99	20.74	0.03	2	1	4	2	142	103	20.38	0.02	2	0	4	1	24	104	21.56	0.24	2	9	3	4
63	105	21.35	0.44	2	1	3	20	103	105	21.20	-0.06	2	4	3	14	119	105	20.86	-2.29	2	4	2	1
18	106	21.20	0.07	2	1	3	1	41	109	20.20	0.00	2	0	4	2	121	110	18.88	0.14	2	0	2	1
33	111	21.23	0.15	2	0	3	1	147	112	20.94	0.05	1	0	2	1	69	113	20.90	0.06	2	1	3	1
101	114	18.14	0.22	1	0	4	2	134	114	19.70	0.03	2	0	4	1	43	115	19.63	0.01	2	1	4	2
115	115	20.17	-0.09	2	7	2	5	77	116	20.60	0.05	2	2	4	6	17	118	20.95	0.05	2	1	3	1
44	120	20.98	0.04	2	7	3	3	52	122	20.09	0.01	2	2	4	1	68	122	20.62	0.04	2	4	4	3
117	123	17.82	0.20	1	0	3	1	90	129	21.04	0.23	2	5	3	2	64	130	20.13	-0.01	2	0	4	2
12	131	21.30	0.13	2	1	3	3	146	131	21.34	0.12	2	0	3	2	47	132	21.05	0.08	2	2	3	2
131	138	20.72	0.72	2	2	3	1	139	138	21.23	0.05	2	3	3	2	117	139	21.73	0.23	2	0	3	10
40	150	21.36	0.12	2	5	3	1	59	153	21.77	0.15	2	3	3	3	147	156	20.89	0.01	1	0	2	0
43	157	20.70	0.06	2	2	4	2	9	158	21.71	0.17	2	2	3	3	28	165	20.49	0.05	2	0	4	7
34	168	20.58	0.03	2	0	4	1	90	171	21.67	0.07	2	0	2	2	137	171	19.23	0.13	2	1	4	2
117	173	20.21	0.01	2	2	4	1	82	174	21.12	0.27	2	2	3	1	91	178	21.45	0.07	2	4	3	13
18	179	20.36	0.01	2	1	4	2	105	181	21.33	-0.01	2	1	2	2	9	182	20.51	-0.02	2	2	4	1
67	184	19.74	0.10	2	1	4	23	93	184	21.68	0.17	2	0	2	4	146	184	20.05	0.00	1	0	2	1
104	190	21.12	0.06	2	4	3	0	119	190	21.45	0.17	2	3	3	1	21	201	20.78	0.02	2	1	4	1
111	204	21.03	0.12	2	3	3	1	133	212	21.47	0.17	2	5	3	5	125	221	20.96	0.08	2	1	3	1
50	224	18.78	0.20	2	1	4	2	139	226	20.34	1.22	2	1	3	4	21	233	21.03	0.12	1	0	2	0
48	233	20.87	0.30	2	1	4	40	77	234	21.84	0.17	2	10	3	7	23	241	19.60	0.17	2	1	4	3
96	241	20.70	0.05	2	0	4	3	80	243	21.96	0.22	2	9	3	4	107	244	20.15	0.04	2	1	4	0
48	246	21.52	0.12	2	3	3	0	58	249	19.99	0.03	2	0	4	4	69	249	20.29	0.03	2	0	4	4
43	250	20.31	0.05	2	1	4	0	61	256	21.36	0.10	2	2	3	2	116	256	21.06	0.12	2	4	3	3
6	261	19.84	0.01	2	1	4	1	17	265	21.14	0.16	2	3	3	2	83	269	18.16	0.23	1	0	4	2

TABLE IV. Magnitudes of NGC 6229 stars.

x (pix)	y	r	g-r	#	$\sigma(r)$ (mag)	#	$\sigma(g)$ (mag)	x (pix)	y	r	g-r	#	$\sigma(r)$ (mag)	#	$\sigma(g)$ (mag)	x (pix)	y	r	g-r	#	$\sigma(r)$ (mag)	#	$\sigma(g)$ (mag)
Field 1								65	8	22.25	-0.15	2	4	4	13	134	18	22.23	-0.10	3	2	5	9
173	23	20.73	0.05	3	2	5	8	127	25	21.39	0.13	3	3	5	11	12	46	22.91	0.09	3	8	4	19
75	48	22.21	-0.48	3	65	5	10	85	52	22.52	0.09	3	4	4	7	109	53	22.84	-0.13	3	1	4	14
145	53	21.98	0.02	3	1	5	10	166	56	20.27	-0.10	3	4	5	7	118	57	23.18	0.00	3	4	4	13
21	58	20.64	0.99	3	4	5	16	106	60	22.29	-0.09	3	2	4	7	193	61	22.40	0.03	2	6	4	7
58	70	22.87	-0.02	3	17	4	13	175	74	22.00	-0.20	3	49	4	58	184	74	23.04	0.09	3	9	4	16
191	75	22.57	0.00	3	3	4	9	125	80	22.29	0.00	3	6	4	9	9	81	23.41	-0.43	3	32	3	5
50	81	22.33	0.18	3	4	4	23	71	85	22.84	-0.85	3	108	5	9	63	87	20.82	0.10	3	2	5	9
132	87	22.12	0.00	3	1	5	13	150	87	22.92	-0.01	3	8	4	7	105	88	22.77	0.04	3	57	4	74
84	91	22.41	-0.01	3	11	4	9	71	96	20.16	0.21	3	4	5	7	58	97	22.29	0.15	3	6	4	7
140	97	23.06	0.09	3	3	3	18	120	99	22.80	0.06	3	2	4	15	40	100	22.44	0.03	3	3	4	9
84	101	22.15	0.12	3	4	4	8	64	102	22.50	0.72	3	3	4	18	111	103	23.04	-0.01	3	16	4	8
54	107	22.56	-0.01	3	34	4	28	115	110	22.59	0.40	3	9	3	39	49	118	22.67	-0.61	3	57	4	11
55	119	22.01	-0.02	2	4	3	6	123	119	22.46	0.04	3	3	4	5	8	121	21.70	0.02	3	3	5	15
67	122	21.52	-0.12	3	12	4	5	153	124	22.42	0.09	3	8	4	3	80	125	21.38	0.03	3	2	5	8
142	125	23.05	0.10	3	12	4	7	13	127	21.76	0.03	3	2	5	7	122	128	22.87	0.17	3	24	4	5
145	135	22.25	-0.01	3	5	4	4	57	138	21.11	0.02	3	4	5	8	116	138	21.82	-0.05	3	8	5	4
151	138	23.04	0.12	3	4	3	6	67	140	21.52	-0.70	3	117	5	9	86	141	22.31	-0.26	3	21	5	5
180	141	23.14	0.09	3	33	3	16	16	142	22.95	0.07	3	21	4	15	77	142	21.85	-0.34	3	53	5	4
48	144	22.30	0.13	3	1	3	2	135	145	22.67	0.06	2	11	4	17	117	149	20.64	0.15	3	3	5	5
155	150	22.83	0.15	3	8	4	7	81	151	21.11	0.03	3	7	5	4	74	152	22.98	0.01	3	18	3	6
35	153	21.37	0.07	3	1	5	10	131	153	23.14	-0.03	3	7	3	12	85	155	20.35	0.22	3	9	3	4
58	157	20.75	0.13	3	3	4	5	173	157	22.78	0.05	3	4	4	16	190	157	21.13	0.00	3	2	5	7
26	158	20.94	0.04	3	13	5	10	116	159	20.48	0.17	3	2	5	6	81	161	21.73	0.09	3	7	5	11
134	161	21.75	-0.01	3	4	5	8	167	163	21.80	0.09	3	67	4	51	50	165	21.70	0.03	2	3	5	7
77	165	21.71	0.06	2	3	5	9	172	165	20.91	0.00	2	3	4	5	94	168	23.04	-0.07	2	16	3	3
22	171	22.34	0.10	3	4	4	10	106	171	22.95	-0.52	3	2	5	45	34	172	23.01	0.23	3	7	3	11
61	172	21.99	0.20	3	61	3	78	138	173	23.24	-0.17	2	11	3	6	163	175	22.55	0.27	3	38	3	37
84	176	21.72	0.00	3	6	5	7	106	176	23.50	-0.24	2	7	3	17	127	177	21.53	0.01	3	1	5	8
4	181	21.18	-0.02	2	5	3	4	78	181	21.86	-0.54	3	81	5	4	46	182	22.56	-1.08	3	19	5	58
157	183	22.92	0.07	3	3	3	11	104	186	23.07	-0.70	3	41	4	10	112	186	22.60	-0.34	3	37	4	4
116	188	22.56	0.29	3	3	3	10	17	189	21.56	0.00	3	6	5	8	165	189	21.84	0.06	3	7	5	4
40	190	22.79	0.10	3	12	4	3	61	190	21.24	0.12	3	8	5	6	116	191	22.46	0.17	3	10	3	12
150	191	20.63	0.19	2	3	5	10	177	191	22.20	-0.35	3	52	5	5	24	195	21.55	0.08	3	4	5	8
76	195	22.06	0.24	3	16	4	7	86	195	22.56	0.15	3	9	4	3	94	195	22.14	0.19	3	34	3	5
99	195	21.72	0.01	2	1	5	11	160	195	21.57	-0.04	3	1	5	6	168	196	22.78	0.07	3	22	4	18
Field 3								166	34	23.05	-0.67	3	93	3	5	146	36	22.49	0.06	3	1	3	2
100	45	22.31	0.09	3	4	3	3	144	48	21.49	0.00	3	2	3	4	161	50	21.70	-0.01	3	1	3	3
10	51	22.65	-0.14	3	10	3	16	126	51	21.82	-0.01	3	3	3	3	119	53	22.92	0.00	3	10	3	7
187	53	21.83	0.04	3	3	3	5	133	59	22.62	0.57	3	5	3	5	173	60	22.24	0.02	3	5	3	4
98	65	19.46	0.20	3	2	3	4	149	70	23.11	-0.25	2	30	3	3	138	72	22.29	0.02	3	1	3	3
188	77	22.88	0.21	3	9	3	4	56	83	22.80	0.09	3	3	3	9	145	84	22.10	-1.15	3	81	3	4
153	96	22.43	0.10	2	6	3	11	135	108	22.43	0.07	2	1	3	4	164	114	21.82	0.09	3	2	3	8
54	115	21.74	-0.01	3	3	3	5	130	121	22.34	0.14	3	3	3	5	190	123	21.09	1.19	3	2	3	5
70	124	22.34	0.03	3	4	3	5	148	126	21.37	0.04	3	1	3	2	59	127	22.97	0.08	3	7	3	4
192	130	21.31	0.01	3	10	3	4	81	132	21.60	0.01	3	3	3	3	159	132	21.22	0.06	3	1	3	5
173	139	22.15	0.05	3	5	3	4	35	141	22.04	-0.01	3	5	3	4	110	141	21.81	0.04	3	2	3	1
13	142	22.40	0.26	3	4	3	3	121	142	22.15	0.14	3	2	3	5	89	151	22.77	0.05	3	13	3	9
144	153	22.42	0.15	3	5	3	4	128	155	22.06	0.06	3	5	3	2	80	157	22.30	0.08	3	5	3	1

TABLE IV. (continued)

x (pix)	y	r	g-r	#	$\sigma(r)$ (mag)	#	$\sigma(g)$ (mag)	x (pix)	y	r	g-r	#	$\sigma(r)$ (mag)	#	$\sigma(g)$ (mag)	x (pix)	y	r	g-r	#	$\sigma(r)$ (mag)	#	$\sigma(g)$ (mag)
32	158	22.99	0.25	3	12	3	13	63	160	22.33	0.01	3	2	3	3	82	163	22.75	0.14	3	6	3	5
136	164	22.65	0.15	3	3	3	3	144	164	22.34	0.07	2	4	3	7	192	166	22.50	0.23	3	4	3	1
171	168	21.65	0.10	3	4	3	6	116	170	22.32	0.16	3	2	3	0	171	173	22.05	-0.02	3	9	3	5
176	173	22.14	0.04	3	4	3	1	160	174	22.18	0.20	3	4	3	4	101	177	21.76	0.08	3	0	3	6
173	179	21.89	0.09	3	3	3	3	67	180	22.85	-0.63	3	45	3	3	192	180	22.79	-0.30	3	65	3	8
126	186	22.42	0.12	3	5	3	2	133	188	21.56	-0.01	3	2	3	4	137	193	21.08	-0.06	2	0	3	5
120	194	21.69	0.02	2	2	3	3	156	194	22.82	0.55	2	6	3	30	192	195	21.82	0.14	3	6	3	4
Field 4								28	4	20.72	0.21	2	6	3	4	99	5	22.55	0.05	2	5	4	3
113	7	22.98	-0.05	3	44	3	9	51	8	22.94	0.24	3	6	3	15	185	8	22.16	0.16	3	5	5	6
195	8	21.37	0.17	3	8	5	7	174	9	20.97	0.13	3	10	5	9	126	11	22.97	0.41	2	4	3	5
137	12	20.90	0.26	3	9	3	2	110	13	19.76	0.25	3	6	5	4	27	15	22.12	0.05	3	6	3	0
131	19	21.33	0.29	3	8	4	3	191	19	20.62	0.14	3	6	5	3	52	20	23.13	0.27	3	15	3	9
103	20	22.57	0.14	3	18	4	0	186	20	20.81	0.35	3	14	4	11	47	21	22.40	0.10	3	6	3	3
158	21	22.18	0.35	3	13	4	9	97	22	22.72	0.18	3	6	4	3	71	24	22.33	0.10	3	6	5	2
78	30	22.25	0.09	3	2	5	4	91	32	23.39	0.26	2	7	3	31	171	32	22.05	0.07	3	7	5	4
131	33	21.32	0.12	3	7	5	4	150	33	22.34	0.42	3	9	4	10	184	35	22.36	0.15	2	9	4	7
51	39	21.84	0.05	3	4	5	3	17	40	21.43	-0.01	3	8	3	5	65	41	21.01	0.10	3	4	5	5
78	41	21.93	0.08	3	4	5	4	180	43	22.81	0.16	3	5	4	3	100	46	22.73	-0.09	3	14	4	2
168	46	22.06	0.14	3	1	5	5	22	48	22.06	0.01	3	3	3	4	90	49	21.41	0.06	3	6	5	15
100	50	22.84	0.15	2	2	4	10	148	50	23.24	0.21	2	18	3	3	121	51	22.04	0.12	3	6	4	21
136	52	23.06	0.22	2	7	3	2	190	54	23.15	0.35	2	26	3	4	150	55	22.95	0.07	3	3	3	4
109	56	22.98	0.03	3	5	4	9	141	58	22.60	0.09	3	9	3	2	169	59	21.34	0.06	3	6	5	4
120	62	22.55	0.03	3	9	4	5	135	62	21.96	-0.03	3	4	5	4	65	63	23.16	0.23	2	6	3	4
93	63	22.96	-0.03	3	8	4	16	141	64	22.23	0.05	3	2	5	6	22	66	22.72	0.19	3	2	3	10
32	67	22.37	0.02	3	8	3	4	130	67	23.25	0.04	2	0	3	4	88	68	22.98	0.47	3	5	3	5
179	68	22.22	0.14	3	5	5	5	151	69	19.40	-0.54	3	5	5	4	170	70	22.54	0.01	3	6	4	5
19	74	21.63	0.05	3	5	3	2	135	76	21.07	0.02	3	6	5	4	124	77	22.06	0.01	2	9	5	5
143	80	22.41	0.01	3	5	5	3	171	81	22.30	0.05	3	11	4	4	31	82	22.11	0.02	3	8	3	5
55	84	22.89	0.07	2	12	3	9	141	88	22.35	0.08	3	8	5	5	159	88	22.84	0.09	3	16	4	6
149	89	23.05	0.05	3	13	4	6	95	93	22.20	0.03	2	5	5	5	181	93	22.98	0.23	3	15	3	9
119	96	19.41	-0.52	2	5	5	5	82	98	22.48	-0.05	3	0	4	6	140	99	22.96	0.07	3	10	4	3
75	104	22.53	0.69	3	10	4	9	186	104	22.29	0.04	3	7	5	8	138	106	23.02	0.17	3	8	4	8
149	110	22.73	-0.12	3	18	4	5	62	111	23.04	0.43	2	2	3	6	133	112	21.34	0.04	3	7	5	3
121	115	21.48	0.01	3	3	5	3	155	115	22.35	0.14	3	8	4	4	77	116	22.38	0.02	3	4	3	4
92	116	23.15	0.26	2	25	3	25	57	118	21.10	0.06	3	5	5	5	115	118	21.24	0.06	3	6	5	3
82	119	21.44	0.05	3	8	5	4	151	119	22.41	0.00	2	1	5	9	49	121	22.53	0.18	3	20	3	5
33	123	23.16	0.02	2	9	3	13	106	125	23.02	0.06	2	5	4	6	129	126	19.91	0.25	3	6	5	5
75	127	22.81	0.08	3	5	4	10	156	130	22.45	0.31	3	16	4	4	23	131	23.05	0.03	3	5	3	5
68	137	20.85	0.15	3	6	5	3	115	137	23.13	0.15	3	9	3	5	196	139	22.29	-0.02	3	4	3	4
157	140	22.52	0.05	3	8	4	3	80	141	20.71	0.18	3	6	5	5	112	143	22.61	0.05	3	4	4	3
155	150	20.34	0.22	3	8	5	5	194	151	21.30	0.02	3	5	5	3	178	153	22.70	-0.01	3	1	4	1
60	155	21.77	-0.03	3	1	5	4	51	157	22.97	0.18	3	2	3	6	128	157	22.84	0.17	2	8	4	9
156	157	21.97	0.03	3	25	5	12	186	158	22.15	-0.01	3	2	5	2	161	159	22.02	0.12	3	6	3	6
168	160	20.83	0.14	3	5	5	3	83	163	21.55	0.01	3	3	5	3	177	163	22.89	0.06	3	16	4	6
55	165	22.63	0.03	3	7	4	7	19	166	22.38	0.06	3	13	3	6	153	166	23.30	0.04	2	7	3	6
63	172	21.98	0.06	3	5	5	6	122	172	21.46	0.01	3	4	5	4	55	174	22.05	0.00	3	0	5	4
174	176	22.75	0.05	3	7	4	4	146	177	22.15	0.18	3	21	4	7	68	179	21.65	0.12	3	6	5	4
99	180	22.88	0.13	3	4	4	4	85	181	23.33	0.06	2	9	3	1	161	191	21.39	0.04	3	8	5	3
Field 5								19	4	21.18	0.00	2	1	5	11	85	4	22.34	0.29	2	0	4	14

TABLE IV. (continued)

x (pix)	y	r	g-r	#	$\sigma(r)$ (mag)	#	$\sigma(g)$ (mag)	x (pix)	y	r	g-r	#	$\sigma(r)$ (mag)	#	$\sigma(g)$ (mag)	x (pix)	y	r	g-r	#	$\sigma(r)$ (mag)	#	$\sigma(g)$ (mag)
32	5	20.81	0.06	3	3	5	6	55	5	23.15	0.19	2	11	3	11	64	6	22.15	0.12	2	9	5	11
118	6	22.21	0.02	3	9	5	5	9	7	22.83	0.13	2	17	4	7	71	7	21.89	0.05	2	6	5	39
124	7	22.20	0.03	3	5	4	4	44	8	22.29	0.13	3	2	5	8	92	8	23.08	0.49	2	16	3	12
37	9	20.55	0.10	3	1	5	6	83	9	22.12	0.13	3	9	5	10	139	9	21.67	-0.02	3	14	5	16
31	10	21.22	0.06	3	1	5	6	63	12	21.65	0.15	3	9	5	12	104	12	21.82	0.14	3	5	5	11
9	13	22.58	0.16	2	14	4	14	110	13	22.60	0.14	3	3	4	13	118	13	22.69	0.04	3	10	4	8
139	13	22.22	-0.37	2	51	4	6	74	14	22.56	-0.06	2	8	3	35	97	14	22.36	0.14	3	7	4	7
40	15	22.86	0.18	3	14	3	9	49	15	22.51	0.21	3	8	4	7	146	17	21.71	0.47	3	2	3	64
32	18	21.93	-0.36	3	59	5	8	79	18	21.48	0.05	3	1	5	7	13	19	21.78	0.06	3	3	5	7
117	19	22.69	0.36	2	6	4	12	24	20	21.95	0.08	3	9	5	9	48	20	21.96	0.02	3	4	5	7
72	20	20.30	0.06	3	38	5	32	123	21	21.77	0.16	3	7	5	40	138	22	22.65	0.06	3	6	4	8
53	24	22.70	0.04	3	35	3	7	130	24	22.23	-0.01	3	19	5	7	62	25	22.48	0.00	3	15	4	17
110	25	19.49	-0.59	3	7	5	7	57	26	22.50	0.08	2	8	3	7	87	26	22.31	0.20	3	8	5	13
80	28	23.20	-0.12	2	3	3	3	23	29	21.99	0.08	3	3	5	5	116	29	21.81	0.03	3	3	5	11
67	30	22.36	0.05	3	5	5	7	123	33	20.37	0.04	3	6	4	5	55	35	21.37	0.03	3	6	5	8
62	35	21.29	0.06	3	7	5	13	95	36	22.66	0.20	2	4	4	9	134	36	23.07	0.24	2	3	4	15
83	38	20.91	-0.08	3	6	5	13	49	39	21.42	0.02	3	2	5	6	105	39	21.28	0.05	3	4	5	8
97	40	22.53	0.12	2	2	4	13	130	40	22.78	0.10	3	18	3	7	17	41	21.72	0.09	3	3	5	7
73	42	21.70	0.13	3	16	5	14	141	42	22.95	0.29	3	13	3	4	31	44	22.17	0.21	2	4	4	6
82	44	20.13	0.22	3	1	5	5	69	46	21.34	0.04	2	0	4	4	92	46	22.87	0.15	3	23	3	41
104	46	22.15	0.08	3	2	5	6	95	49	22.86	0.09	2	18	4	11	17	50	22.73	0.10	3	10	4	11
32	50	21.80	0.14	3	5	5	8	39	52	22.29	0.04	3	10	5	12	46	52	22.50	0.48	2	0	4	16
71	52	22.16	-0.09	3	21	5	8	113	52	19.69	0.22	3	4	5	4	10	53	22.07	0.06	2	0	5	10
56	53	22.43	0.08	3	2	5	9	105	53	22.38	0.03	3	4	4	8	143	53	22.04	0.25	3	6	4	6
21	55	22.70	0.14	3	9	4	10	127	55	21.06	0.03	3	5	5	6	95	56	21.21	0.06	3	3	5	6
82	57	22.22	0.01	3	8	5	7	52	58	22.81	0.20	3	8	4	10	33	60	21.78	0.00	3	5	5	6
41	60	22.08	0.00	3	5	5	6	78	63	22.71	0.00	3	12	4	10	14	64	23.35	0.13	2	7	3	9
138	65	22.49	0.60	3	23	3	8	53	67	22.97	0.51	2	8	3	22	66	67	22.56	0.08	3	9	4	13
89	67	23.30	0.41	2	3	3	3	124	70	22.84	0.18	2	1	3	3	33	72	21.39	-0.01	3	5	5	7
44	73	22.53	0.07	3	13	4	4	129	73	22.49	0.14	3	8	4	10	35	77	22.89	0.10	2	9	4	11
77	80	21.81	-0.04	2	3	5	5	26	82	22.90	0.18	2	1	4	4	50	82	21.60	-0.01	3	7	5	5
92	82	21.88	0.13	3	4	5	8	129	82	22.10	0.19	2	8	4	2	135	83	20.74	0.23	3	4	5	7
65	86	22.75	0.06	3	7	4	12	76	94	21.62	0.03	3	6	4	8	137	96	22.60	0.65	3	18	3	11
33	107	22.15	0.31	3	16	5	18	50	108	20.84	0.14	3	1	5	5	37	109	22.30	0.20	3	19	4	8
26	110	21.70	0.01	3	5	5	7	74	111	22.11	0.13	2	26	5	9	119	112	22.24	0.41	3	4	4	11
113	114	20.69	1.18	3	1	5	6	17	117	22.92	0.00	2	4	3	6	36	118	23.10	0.18	2	0	3	4
55	122	20.43	0.21	3	2	5	5	21	123	22.64	0.12	3	9	4	13	105	125	22.41	0.01	3	2	5	8
57	127	21.90	0.07	2	5	4	6	6	131	22.58	0.09	2	0	4	10	61	131	20.88	0.09	3	3	5	4
49	133	22.79	0.21	2	1	4	10	139	137	23.07	0.02	3	9	3	7	14	142	22.95	0.14	3	10	3	11
68	142	22.86	0.06	3	14	4	8	88	146	23.39	-0.19	2	34	3	9	23	149	21.82	0.04	3	5	5	12
100	149	21.17	0.03	3	2	5	4	131	150	21.53	0.05	2	8	4	4	30	152	20.74	0.15	3	4	5	3
116	154	22.39	0.22	3	2	3	2	70	159	21.90	0.03	3	4	5	6	110	159	21.74	0.00	3	2	5	5
28	160	22.21	-0.05	3	13	5	7	43	161	22.09	0.07	3	8	5	9	28	166	21.90	0.05	3	9	5	6
131	167	21.79	-0.22	3	37	4	7	33	171	23.08	-0.07	3	10	3	5	137	171	22.51	0.23	3	4	4	12
75	175	23.06	-0.08	2	20	3	7	7	179	22.37	0.12	2	3	5	8	80	182	23.35	0.07	2	8	3	13
125	186	21.33	0.00	3	3	5	4	80	189	22.29	-0.01	3	8	5	6	90	193	21.97	-0.06	3	6	5	4
Field 6								29	9	22.28	-0.01	2	12	5	5	46	14	22.74	0.64	3	19	3	10
160	37	22.95	0.05	3	21	4	13	185	37	21.79	0.65	3	4	4	12	39	48	22.89	0.01	2	6	4	6
34	55	22.41	0.17	2	16	4	7	13	59	21.75	0.09	3	3	5	7	147	61	21.96	-0.05	3	11	5	8

TABLE IV. (continued)

x (pix)	y	r	g-r	#	$\sigma(r)$ (mag)	#	$\sigma(g)$ (mag)	x (pix)	y	r	g-r	#	$\sigma(r)$ (mag)	#	$\sigma(g)$ (mag)	x (pix)	y	r	g-r	#	$\sigma(r)$ (mag)	#	$\sigma(g)$ (mag)
74	62	21.82	0.43	3	7	5	11	158	68	22.43	-0.02	3	9	5	9	23	69	22.57	0.43	3	24	4	13
117	77	21.53	-0.03	3	7	5	7	69	80	21.66	0.00	3	3	5	6	138	81	22.79	0.10	3	7	4	10
50	82	23.05	0.10	3	8	4	11	101	82	22.08	0.04	3	4	5	7	145	99	22.93	0.08	3	13	4	11
118	105	21.91	0.06	3	4	5	12	94	106	23.19	0.03	3	2	3	18	66	112	22.53	0.24	3	9	4	17
47	113	23.13	0.25	2	4	3	18	78	115	22.17	-0.36	3	19	5	88	58	117	22.78	0.10	3	15	4	9
158	118	21.81	0.03	3	6	5	8	83	119	20.57	0.20	3	3	3	4	23	121	22.44	0.06	3	3	4	6
9	122	22.79	0.14	3	12	4	9	123	126	23.08	0.24	3	20	3	11	90	131	21.95	0.08	3	4	4	8
104	134	20.12	0.28	3	4	5	7	51	138	22.90	0.02	3	12	4	6	141	138	22.00	0.03	3	6	5	9
155	143	22.86	0.27	3	8	3	9	57	144	23.10	-0.07	3	44	4	9	9	145	23.11	0.24	2	0	3	11
50	146	22.09	0.15	3	2	5	13	175	147	23.22	0.19	3	17	3	15	157	150	23.00	0.13	3	9	4	20
103	152	22.27	0.22	2	8	3	6	81	156	21.81	0.09	3	5	5	8	189	157	20.25	0.27	2	4	4	6
22	158	21.40	0.10	3	3	5	7	118	158	21.46	0.12	3	3	5	9	77	163	22.66	0.06	3	7	3	7
126	163	22.68	0.08	3	12	4	14	183	163	22.74	0.24	3	3	3	8	67	164	22.40	0.14	3	7	4	11
144	166	21.91	0.05	3	5	5	6	61	170	21.20	0.14	3	2	5	6	54	173	22.42	0.13	3	6	4	8
121	174	22.55	0.00	3	5	4	9	153	175	23.23	-0.19	3	39	4	8	108	176	22.44	0.42	3	2	4	23
140	178	22.66	0.19	3	8	4	8	41	180	21.57	0.09	2	0	5	9	15	181	23.11	0.14	2	4	3	12
49	181	22.32	0.10	3	8	4	4	105	182	22.10	0.82	3	6	4	5	66	184	22.36	0.14	3	4	4	8
44	187	22.85	0.22	3	13	4	5	51	187	22.73	0.12	3	10	4	8	88	188	21.69	0.12	3	2	5	10
17	191	21.83	0.18	2	1	5	6	68	191	22.62	-0.97	3	136	5	6	167	194	22.59	0.07	3	11	4	7
162	196	22.34	0.06	2	2	4	11																

outskirts of NGC 7006 are shown in Fig. 8. The solid line is the mean subgiant locus from Fig. 7. The main-sequence turnoff has been detected in all three clusters.

Figure 9 shows the NGC 5466 data transformed to the B,V system using the equations given in Sec. II. The thick, solid line is the mean locus of the faintest stars in the photographic survey by Buonanno *et al.* (1984). They obtained a color-magnitude diagram of NGC 5466 that reaches to $B = 19$ mag but relies on transformations of P,V photoelectric photometry of nine stars in the field of this cluster by Cuffey (1961) to define the magnitude system. The giant branches in both studies merge smoothly together in color. Buonanno *et al.* (1984) review the metallicity and reddening determinations for NGC 5466. $E(B-V)$ is known to be less than 0.03 mag, while published [Fe/H] values range from -2.2 to -1.5 dex; the median of the ten published determinations, not all of which are independent, is -1.9.

We adopt for all the clusters the distance moduli $(m-M)_V$ tabulated by Harris and Racine (1979), which assume M_V (RR Lyraes) = 0.6 mag as well as their tabulated reddening value $E(B-V) = 0.05$ mag for NGC 5466. We then superpose onto the NGC 5466 c-m diagram the 16×10^9 yr isochrone for $Z = 10^{-4}$ and helium content $Y = 0.20$ from VandenBerg and Bell (1985). The isochrones near the main sequence are somewhat bluer (by about 0.08 mag) than the locus of stars in very metal-poor clusters (including M92) with adequate photometry. However, the turnoff luminosity itself of NGC 5466 requires an age of at least 16×10^9 yr, comparable to that of the globular clusters in the inner halo. There is no sign that NGC 5466 is younger than the average globular cluster.

It is possible that the color discrepancy between the isochrones and the clusters $B-V$ colors near the turnoff result from a problem in the theoretical isochrones, as several of the metal-poor clusters in VandenBerg's (1983) Fig. 5 (as well as all three clusters studied in this paper) show the same phenomenon. However, the use of accurate model atmospheres in VandenBerg and Bell (1985) should have eliminated any significant error in color. It is also possible that the photometric errors are larger than we believe, although this too seems unlikely. A more reasonable explanation for at least part of the color discrepancy lies in our neglect of the metallicity dependence in the transformation from $g-r$ to $B-V$ color. The effective wavelengths of g and r (4930 and 6650 Å, respectively) are both redder than that of B at about 4400 Å. Although the standards defining the Thuan-Gunn system are white dwarfs and metal-poor subdwarfs, their mean metallicity is higher than that of the metal-poor globular clusters discussed in this paper; neglecting the reduced line blanketing throughout the B filter bandpass in the globular cluster stars will lead to $B-V$ colors for them that are too red. The fact that the $B-V$ colors of the M3 stars predicted from our measured $g-r$ colors were in the mean 0.085 mag redder than those measured by Sandage (1970) (see Sec. II*b*) supports this hypothesis. One should also note that the transformation given by Kent (1985) between $g-r$ and $B-V$ colors derived from photometry of stars with near solar metallicity has even redder $B-V$ colors for a given $g-r$ color than do the equations used in this paper and derived directly from the bright standards of the Thuan-Gunn system, which are somewhat metal poor in the mean.

Ideally, $B-V$ must be determined from a color that more closely spans the B and V wavelength bandpasses (i.e., $v-g$ in the Thaun-Gunn system), rather than be extrapolated from a continuum slope defined at longer wavelengths only. It would also be desirable for the VandenBerg and Bell (1985) isochrones to be converted into the Thuan-Gunn system, since this photometric system is finding widespread use with CCD detectors.

The B, V c-m diagram of NGC 6229 is shown in Fig. 10.

TABLE V. Magnitudes of NGC 7006 stars.

x (pix)	y	r	g-r	#	$\sigma(r)$ (mag)	#	$\sigma(g)$ (mag)	x (pix)	y	r	g-r	#	$\sigma(r)$ (mag)	#	$\sigma(g)$ (mag)	x (pix)	y	r	g-r	#	$\sigma(r)$ (mag)	#	$\sigma(g)$ (mag)
Field 1								77	4	22.51	0.23	1	0	3	8	98	5	21.70	0.31	2	2	4	4
42	7	23.28	0.39	2	19	3	9	144	7	22.02	0.09	2	5	4	2	154	7	22.29	-0.08	1	0	4	17
10	8	23.14	0.36	1	0	2	1	133	8	20.73	0.27	2	1	4	2	150	8	23.05	-0.82	2	20	2	5
21	9	23.45	0.42	2	11	3	28	28	11	22.71	0.13	2	18	3	5	50	11	22.63	0.17	2	2	3	15
154	11	23.07	-0.31	2	5	2	35	34	13	22.90	0.30	2	11	2	1	110	13	21.93	0.12	2	8	4	2
19	17	22.49	0.16	2	8	4	6	66	17	22.76	0.21	2	14	2	11	82	18	22.30	0.16	2	6	4	1
12	19	23.44	0.20	1	0	3	26	31	21	21.84	-0.06	2	1	4	3	8	27	22.86	0.29	2	0	3	11
149	29	23.36	0.26	2	10	3	12	106	30	23.13	0.38	1	0	3	14	122	30	23.38	0.46	1	0	2	17
52	32	22.72	0.22	2	3	4	11	112	32	23.35	0.29	1	0	2	4	131	32	22.72	0.19	2	8	3	6
37	35	23.08	0.21	2	10	4	30	144	37	22.56	0.23	2	1	4	4	71	39	23.06	-0.01	2	25	3	9
45	40	21.90	0.19	2	4	4	5	68	47	23.25	0.24	2	19	2	3	47	48	22.93	0.38	2	2	3	8
38	49	22.77	0.21	2	1	4	8	99	49	23.31	-0.32	2	50	3	6	82	50	21.81	0.21	2	0	4	4
130	50	19.81	0.31	2	4	4	0	62	57	23.37	0.34	1	0	3	7	45	61	23.36	0.35	2	16	2	23
99	61	23.30	0.61	1	0	3	40	140	61	23.31	0.39	2	4	3	14	135	65	22.80	1.15	2	1	2	6
149	66	23.24	0.29	1	0	2	7	71	67	19.83	1.13	2	2	4	3	85	67	22.64	0.21	2	0	4	10
36	79	23.48	0.49	2	16	2	41	56	79	18.95	0.09	2	3	4	1	94	84	22.82	1.37	2	5	2	0
127	84	22.32	0.21	2	1	4	9	72	86	22.98	0.10	2	18	3	6	41	87	23.14	0.39	2	10	3	12
35	89	23.49	0.52	1	0	2	21	140	89	23.19	0.34	1	0	3	13	39	91	23.47	0.26	1	0	2	34
107	97	23.12	0.31	2	21	3	8	31	98	22.27	0.09	2	8	4	9	101	100	22.92	0.20	2	10	4	17
13	101	21.19	0.50	2	0	4	25	9	106	22.07	0.08	2	6	3	10	22	108	23.45	0.23	1	0	3	10
72	108	22.88	0.20	2	11	3	15	40	119	23.24	0.67	2	5	2	15	116	119	22.89	0.85	2	10	3	14
7	126	21.75	0.13	2	1	4	2	109	132	22.38	0.20	2	8	4	20	26	135	22.68	0.06	2	2	4	10
72	140	23.07	0.01	2	2	3	4	64	146	19.61	0.31	2	2	4	2	115	151	21.71	0.83	2	4	4	11
9	156	22.21	0.13	2	2	4	12	86	156	21.64	1.17	2	1	4	4	64	158	22.52	0.13	2	5	4	2
29	159	23.19	0.54	1	0	3	26	19	167	18.80	0.15	2	2	4	22	37	182	21.73	0.16	2	4	4	2
77	183	22.23	0.07	2	7	4	7	70	184	23.21	-0.09	2	2	4	33								
Field 2								77	8	21.54	0.23	2	5	3	3	82	17	19.87	0.19	2	3	3	1
115	43	23.07	0.27	1	0	3	10	37	45	23.45	0.40	1	0	2	17	67	47	23.28	0.21	1	0	3	9
104	47	22.72	1.66	2	8	2	20	57	66	19.45	1.41	2	4	3	2	89	66	22.53	1.85	2	4	2	14
12	68	22.97	0.12	1	0	3	2	126	68	22.83	0.44	2	9	3	4	21	69	20.29	0.63	2	5	3	2
6	70	21.18	1.51	2	7	3	9	116	78	23.38	1.43	1	0	2	4	38	95	22.43	1.55	2	4	2	14
13	126	22.34	1.32	2	5	3	15	66	139	20.63	1.11	2	4	3	2	86	142	23.48	0.50	1	0	3	13
19	146	20.89	0.32	2	3	3	3	41	159	19.09	0.88	2	5	3	3	63	161	21.62	0.23	2	1	3	5
79	163	22.94	0.24	2	9	3	1	53	176	20.79	0.85	2	4	3	3	9	193	21.56	0.20	2	2	3	0
Field 3								98	13	21.07	1.11	2	3	3	1	114	16	21.19	0.37	2	3	3	1
139	17	22.65	0.07	1	0	3	5	25	22	19.46	1.33	2	0	3	0	89	28	21.43	0.39	2	0	2	0
77	30	21.47	0.43	2	0	3	2	116	34	22.95	0.42	1	0	3	9	100	48	20.45	0.77	2	0	3	1
23	52	22.61	0.27	2	1	3	7	14	68	22.58	0.30	1	0	3	7	64	70	23.47	0.34	1	0	3	17
109	72	23.19	0.39	1	0	3	7	145	73	23.02	0.31	1	0	3	4	64	82	20.13	1.44	2	1	3	1
147	87	23.30	0.16	1	0	3	6	11	92	22.35	0.20	2	2	3	1	143	97	23.01	0.20	1	0	3	6
34	102	22.90	1.10	1	0	2	38	96	106	23.25	0.24	1	0	2	4	90	108	21.01	0.37	2	0	3	2
23	120	19.96	0.69	2	0	3	0	97	134	19.21	-0.26	2	1	3	1	126	138	22.60	1.42	1	0	3	21
148	138	23.24	0.17	1	0	3	6	116	146	23.32	0.21	1	0	3	14	135	148	20.78	0.68	2	1	3	5
29	171	20.80	0.86	2	0	3	1	101	172	22.99	0.06	1	0	3	12	145	175	21.08	0.28	2	2	3	2
123	182	23.35	0.52	1	0	2	18	55	201	21.91	1.49	2	1	3	5	80	215	21.10	1.26	2	1	3	6
50	222	22.44	1.37	2	0	3	12	24	227	22.51	1.25	2	2	3	13								

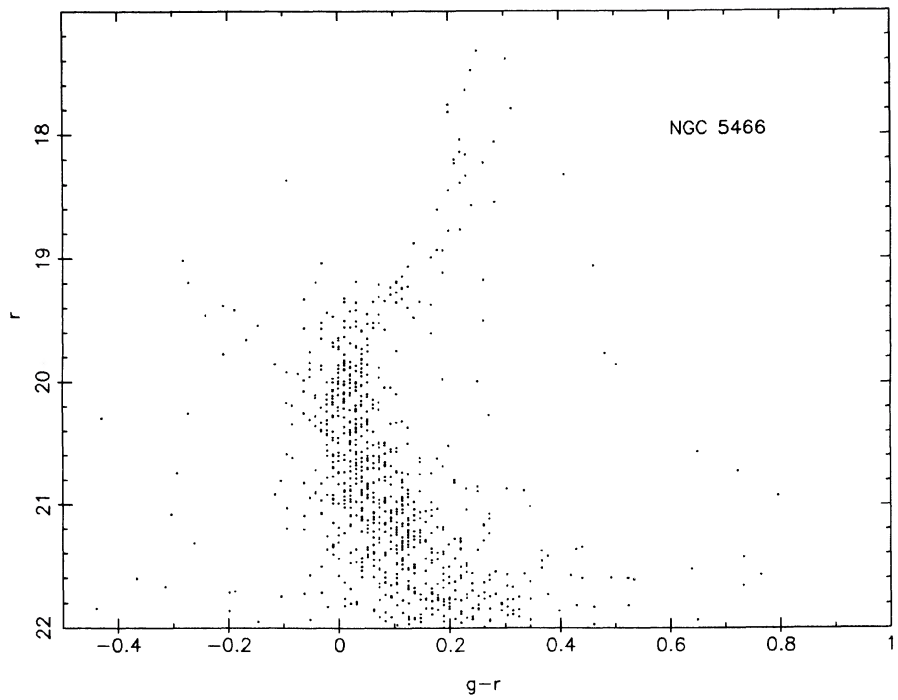

FIG. 4. The *g,r* color-magnitude diagram for stars in NGC 5466 measured on at least two of the *g* frames is plotted.

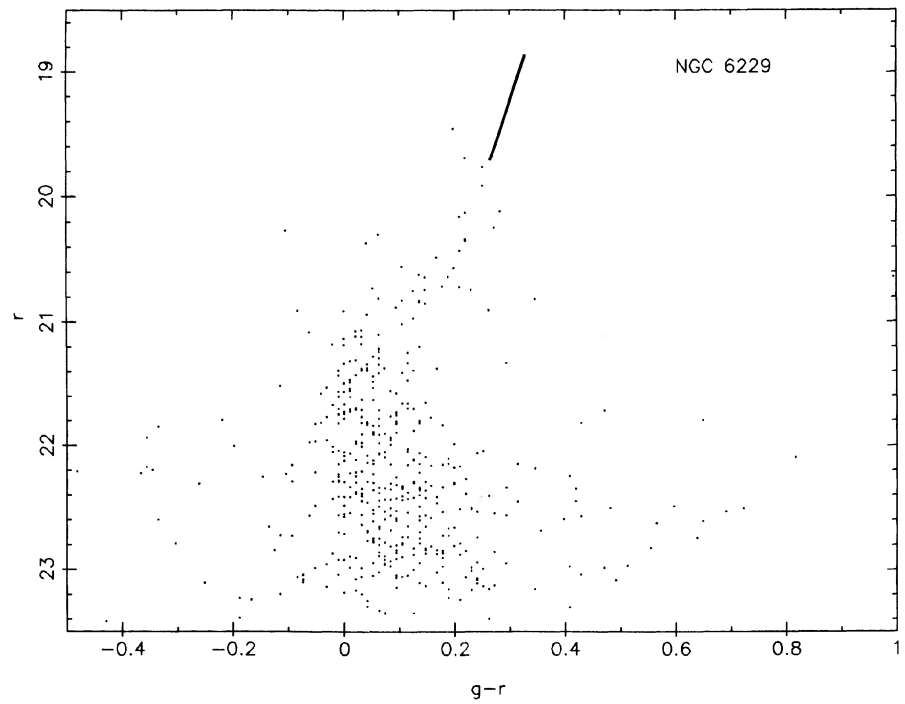

FIG. 5. The *g,r* color-magnitude diagram for stars in NGC 6229 detected on at least three of the *g* and two of the *r* frames is shown. The solid line is the mean locus of bright giants from Fig. 6.

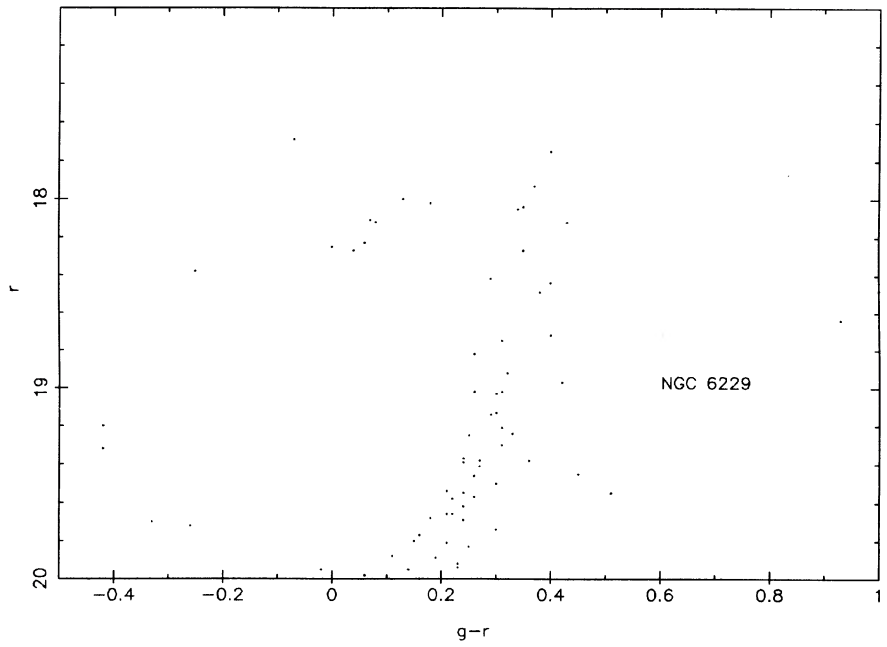

FIG. 6. *g,r* c-m diagram for stars in a field close to the center of NGC 6229.

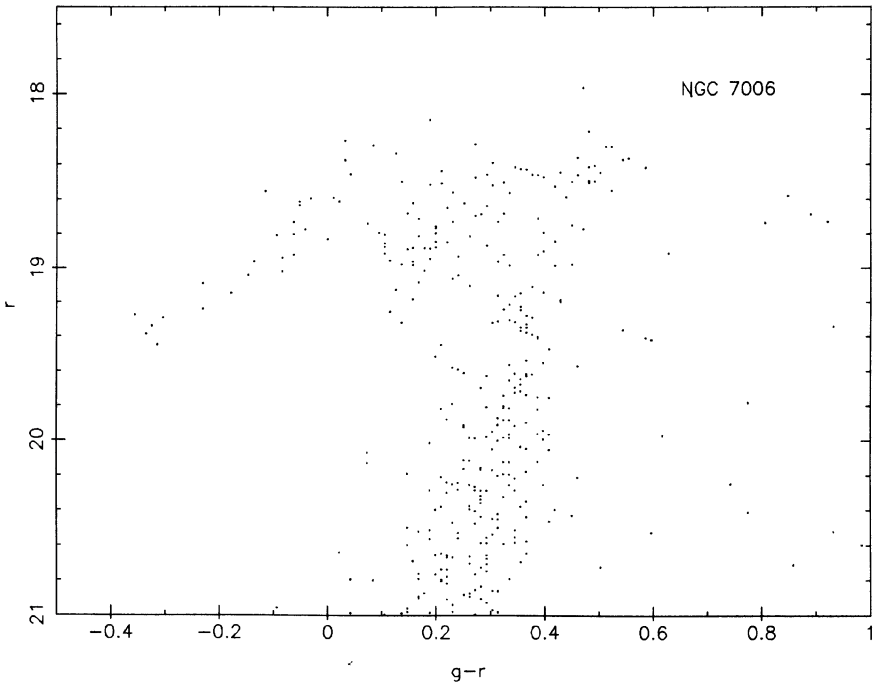

FIG. 7. *g,r* color-magnitude diagram for a region close to the center of NGC 7006.

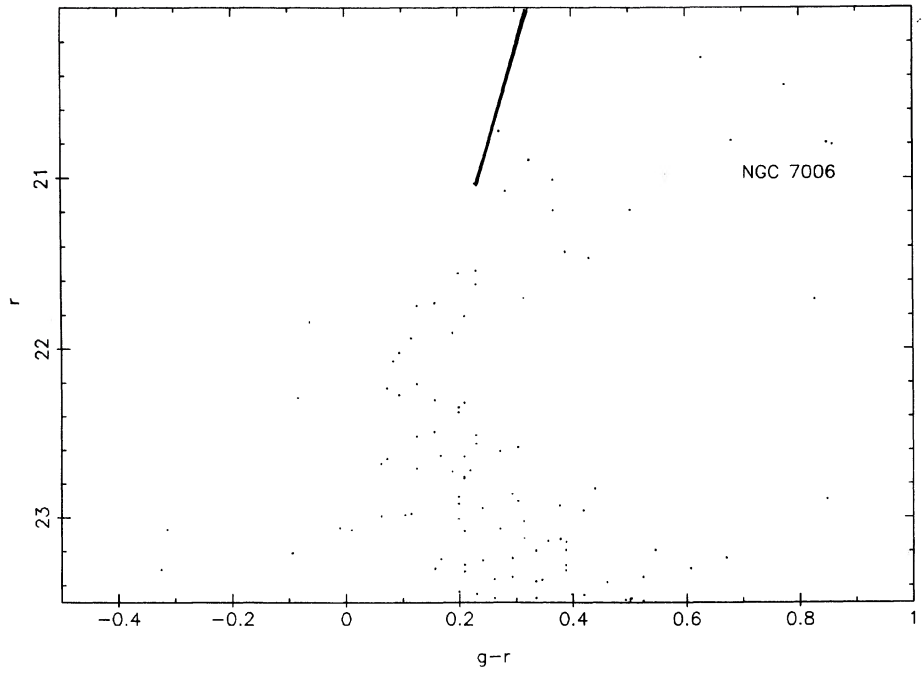

FIG. 8. *g,r* c-m diagram for stars in the three outlying fields of NGC 7006 measured on at least two of the *g* frames.

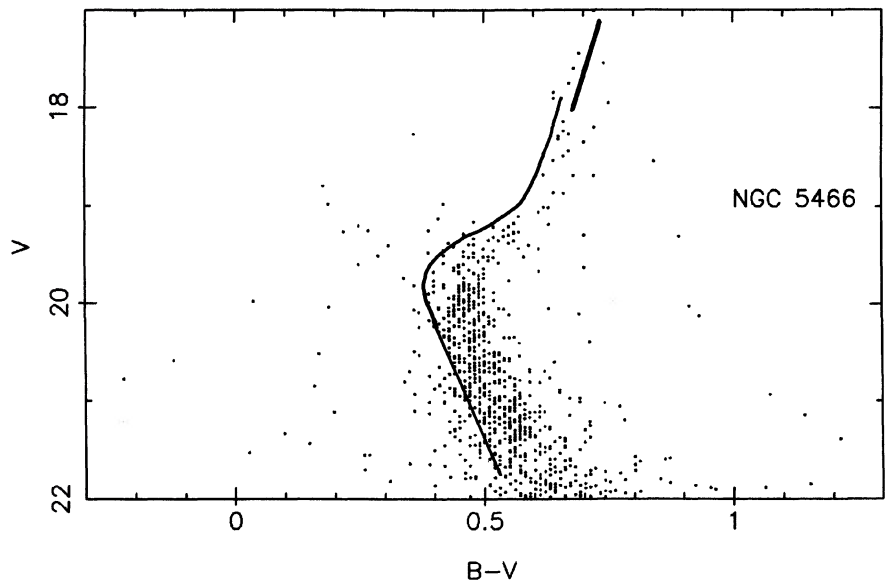

FIG. 9. *B,V* color-magnitude diagram for NGC 5466. The thick, solid line is the mean locus of the bright giants from Buonanno *et al.* (1984). The thin solid line is the isochrone of VandenBerg and Bell (1985) for $Z = 10^{-4}$, $Y = 0.20$, and age $= 16 \times 10^9$ yr.

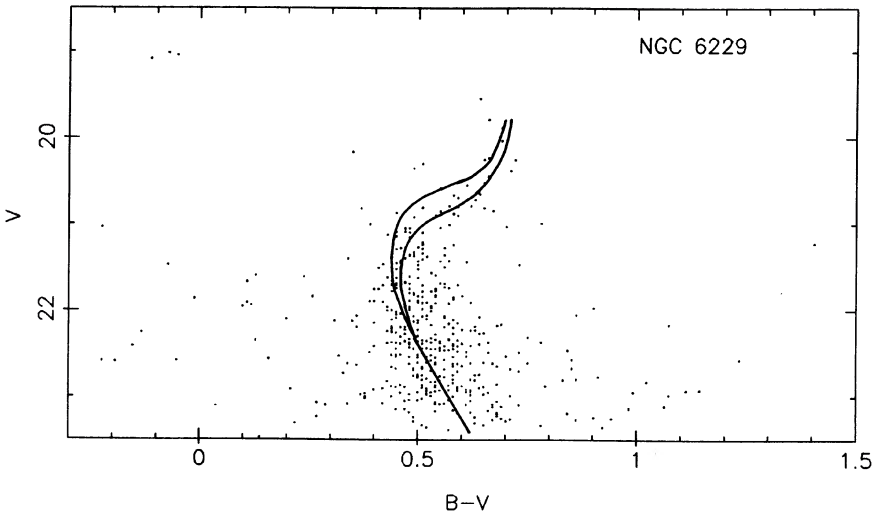

FIG. 10. B,V color-magnitude diagram for NGC 6229. The thick, solid line is the mean locus of the brighter giants from our frames. The thinner lines represent isochrones with ages of 14 and 18 billion years with $Z = 3\times10^{-4}$ and $Y = 0.20$ from VandenBerg and Bell (1984) offset 0.10 mag redder in $B - V$.

Metallicity determinations for NGC 6229 are reviewed by Pilachowski (1983); they range from [Fe/H] = -1.3 to -1.5 dex. Zinn (1980) found $E(B - V) = 0.01$ mag, and a very low reddening is supported by the relevant entries near NGC 6229 from Burstein and Heiles' (1983) compilation of H I column densities along the line of sight to galaxies. Superposed on Fig. 8 are isochrones from VandenBerg and Bell (1984) (basically differing only in detail from those of VandenBerg 1983) for a helium content $Y = 0.20$ and $Z = 3\times10^{-4}$ and for ages of 14 and 18 billion years. These isochrones have been offset to redder $B - V$ colors by 0.10 mag to produce a reasonable fit. The deduced age is 17 ± 3 billion years, comparable to those of the nearer galactic globulars discussed by VandenBerg (1983).

The $B - V$ c-m diagram for the three outlying fields in NGC 7006 is shown in Fig. 11. The thick, solid line is the mean location of the subgiants from the sample in the inner part of the cluster. The metallicity of NGC 7006 has been measured from low-resolution spectra of individual stars by several authors, including Searle and Zinn (1978) and Cohen and Frogel (1982). A mean value of [Fe/H] = -1.7 dex with respect to the Sun is adopted here. Therefore the $Z = 3\times10^{-4}$ and $Y = 0.20$ isochrones for ages of 14 and 18 billion years from VandenBerg and Bell (1985) are shown as the thin, solid line in the figure. The 18×10^9 yr isochrone was shifted 0.10 mag to the red in $B - V$ color to yield the dashed line (which is identical to the isochrone fit to NGC 6229) in Fig. 9. This isochrone produces a satisfactory fit for both clusters. The age of NGC 7006 is therefore 17 ± 2 billion years. The claim by Carney and Inman (1982) and Carney (1984) of an unusually bright turnoff in NGC 7006, and hence an age significantly below that of most globular clusters, is spurious. (The age uncertainties quoted up to this point reflect only the observational uncertainties in the photometry and the sampling statistics of small numbers of stars, particularly in NGC 7006.)

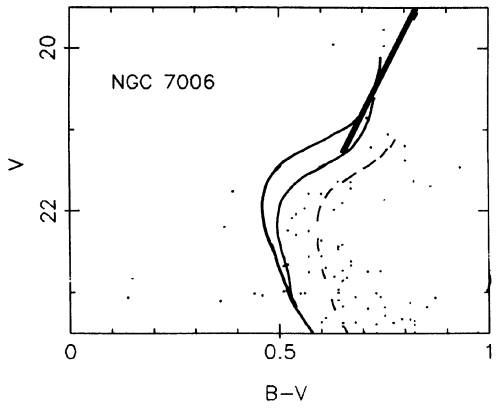

FIG. 11. B,V c-m diagram for NGC 7006. The thick solid line is the mean locus of the bright giants from our frames. Isochrones of age 14 and 18×10^9 yr with $Z = 3\times10^{-4}$ and $Y = 0.20$ from VandenBerg and Bell (1985) are shown as the thin lines. The dashed line is the 18×10^9 yr isochrone shifted 0.10 mag redder in $B - V$.

Globular cluster ages determined by main-sequence fitting are also sensitive to errors in metallicity and helium abundance. Iben (1971) gives approximations for the dependence of the age deduced from the turnoff luminosity on these two parameters. If the uncertainty in metallicity is ± 0.3 dex and in the helium abundance is ± 0.05, then the resulting uncertainties in age are $\pm 7\%$ and $\pm 10\%$, respectively, for a cumulative uncertainty (including the observational one) of $\pm 17\%$ in the cluster age. This does not yet include the errors in the theoretical calculations of the isochrones, which are discussed in many references (see, for example, Flannery and Johnson 1982).

b) Luminosity Functions

We have seen that isochrone fitting requires a shift in color of about 0.10 mag between the observed and theoretical main sequences. The origin of this problem could be in the data, in the theoretical evolutionary tracks for low-mass metal-poor stars, or in the transformation of $g - r$ to $B - V$ colors. However, the existence of the turnoff itself is obvious in the data, both in color and in relative numbers of stars at various luminosities. One can therefore use the luminosity function as suggested by Paczynski (1984) to determine cluster ages, since presumably the theoretical luminosities are

more accurate than the colors, and the transformation from calculated to observed parameters is more straightforward. Even if one does not trust the theoretical calculations, relative ages for several clusters of similar metallicity (such as the three studied here) can be obtained since reliable distance moduli are available from RR Lyrae variables in each cluster.

Since our detection criteria, at least within the small outlying fields, are not affected by crowding, and all stars brighter than the limiting magnitude of the tables have been counted, the necessary data for constructing luminosity functions are available (Table VI). Stars were counted in bins 0.2 mag wide in g in the outlying fields of each cluster. Counts were also done in the more crowded inner fields for NGC 6229 and NGC 7006, where the magnitude limit was set brighter by an amount sufficient to avoid missing any stars, although the magnitudes themselves in these more crowded fields have 0.10 mag uncertainties. In the outlying fields of NGC 7006, an approximate correction for field stars was made only to the faintest four bins by eliminating stars with $B - V \geqslant 0.85$ mag. This is undoubtedly a slight underestimate of the actual field-star contamination; in particular some of the brightest stars in the outlying fields are also probably not members of NGC 7006.

The luminosity functions for NGC 6229 and NGC 7006 were assembled by forcing the bright counts to fit smoothly onto the deeper ones in each cluster. The derived luminosity function for NGC 7006 is shown in Fig. 12, where the luminosity function of the bright stars from the inner fields is indicated by the dashed line. The luminosity function of NGC 5466, which is well defined and smooth because of the large number of stars counted, is shifted horizontally by δDM (5466–7006), the difference in distance modulus between NGC 5466 and NGC 7006, and vertically by forcing good agreement at intermediate magnitudes ($20 \leqslant g \leqslant 21.5$ mag in NGC 7006) to remove the effect of the difference in the number of stars counted. The scaled luminosity function of NGC 5466 for δDM (5466–7006) of 2.6 mag is shown as the solid line, while the short-dashed line (which coincides with the solid line when it is not separately drawn) indicates the luminosity function of NGC 5466 for δDM (5466–7006) = 1.8 mag. The NGC 7006 counts (indicated by points), corrected for field stars (the asterisks), demonstrate that the best fit is δDM (5466–7006) = 2.2 mag. Although the statistical uncertainties arising from the small number of stars counted in NGC 7006 are apparent in Fig. 11, the cluster's luminosity function supports δDM (5466–7006) = 2.2 ± 0.2 mag. The true value of δDM (5466–7006) as determined from RR Lyrae variables in each cluster is 2.16 mag. Unfortunately, the limited number of stars counted and the uncertain field-star corrections do not allow a more stringent limit on age differences to be set than that corresponding to a maximum difference in turnoff luminosity of 0.2 mag between NGC 5466 and NGC 7006, equivalent to a maximum age difference of + 25%, − 20%.

The luminosity function of NGC 6229 is better determined due to the larger number of stars counted. We find δDM (5466–6229) = 1.6 ± 0.1 mag. The true value of the difference in distance moduli is 1.54 mag, which should be increased by about 0.1 mag to allow for the slightly higher metallicity of NGC 6229 than NGC 5466. (The correction follows from the approximate parametrizations of the dependence of ages deduced from turnoff luminosities on metallicity by Iben 1971.) Thus the age difference between NGC 6229 and NGC 5466 must be less than 10% of 18×10^9 yr.

Although no use is made here of Paczynski's (1984) theo-

TABLE VI. Luminosity functions.

Bin center g (mag)	NGC 5466 #	NGC 6229 (bright) #	NGC 6229 (faint) #	NGC 7006 (bright) #	NGC 7006 (faint) #	Faint-field #
17.3	0	0	0	0	0	
17.5	1	1	0	0	0	
17.7	2	0	0	0	0	
17.9	3	0	0	0	0	
18.1	1	7	4	0	1	
18.3	7	5	0	1	0	
18.5	5	2	1	1	0	
18.7	6	3	0	7	1	
18.9	5	2	2	17	3	
19.1	6	5	1	10	3	
19.3	22	7	2	3	0	
19.5	28	11	0	8	0	
19.7	25	8	1	6	0	
19.9	44	15	2	10	3	
20.1	53	14	2	11	4	
20.3	52	24	4	5	1	
20.5	55	24	4	14	3	
20.7	66	15	9	15	2	
20.9	71	6	16	38	2	
21.1	74	0	17	33	2	
21.3	77	0	18	35	4	
21.5	74	0	32	51	4	
21.7	61	0	35	62	5	
21.9	77	0	46	59	8	
22.1	71	0	42	64	8	
22.3	36	0	48	63	11	
22.5	36	0	70	62	16	
22.7	16	0	45	47	12	
22.9	2	0	69	20	14	
23.1	2	0	55	15	19	
23.3	0	0	53	11	16	
23.5	0	0	46	7	26	24
23.7	0	0	33	9	33	30
23.9	0	0	21	14	32	24
24.1	0	0	5	6	26	20

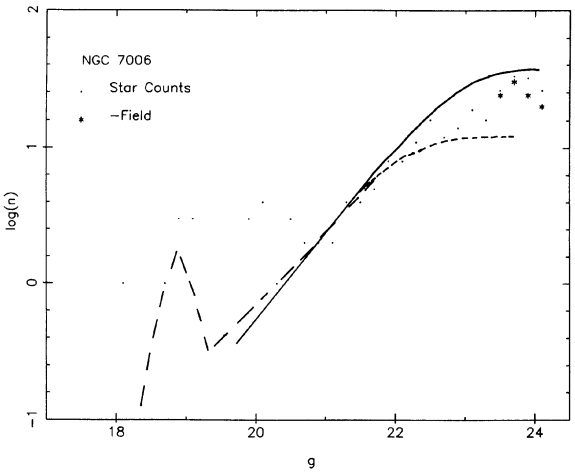

FIG. 12. The logarithm of the number of stars in bins 0.2 mag wide in the fields on the outskirts of NGC 7006 is indicated as a function of g magnitude by dark circles. The asterisks are the star counts corrected for field-star contamination. The dashed line is the luminosity function derived for the brighter stars from fields closer to the center of the cluster. The solid line is the NGC 5466 luminosity function shifted for a difference in distance modulus between that cluster and NGC 7006 of 2.6 mag, while the short-dashed line is for a difference of 1.8 mag.

retical predictions for luminosity functions, the shape of the luminosity functions derived from the star counts is similar to that predicted. For nearby clusters where adequate numbers of stars can be obtained without excessive field-star contamination, the technique of age dating via luminosity functions shows great promise.

c) The Horizontal Branch

The horizontal branch (HB) of NGC 5466 is illustrated in the study of Buonanno *et al.* (1984). It is quite blue, but without the extended tail of extremely hot, blue stars shown by M92 or M15. The mean color of the HB in NGC 5466 is normal for a cluster of its own metallicity. NGC 7006, on the other hand, is the paradigm of the "second parameter" effect described by Sandage and Wildey (1967), where the HB is unusually red for the metallicity of the cluster. Our c-m diagram for NGC 7006 (Fig. 7) shows an HB identical to that of Sandage and Wildey; there is no evidence for a tail of extremely blue stars, which would have been below the magnitude limit of their data. The morphology of the HB of NGC 6229 is shown for the first time in Fig. 6. It is an unusually red HB for a relatively metal-poor cluster, with a mean color, including any RR Lyrae variables, of about $B - V = 0.5$ mag. Thus NGC 6229 is an even more extreme example of the second parameter problem than is NGC 7006. Freeman and Norris (1981) point out that the problem of anomalous HB color distribution is not confined exclusively to the classical second-parameter clusters in the outer halo. The distribution of stars in color along the HB is quite different even between well-studied nearby clusters of similar metallicity such as M92 and M15, where the mean color of the HB may be almost identical.

A theoretical review of the factors influencing the color distribution along the HB in globular clusters has been given by Renzini (1977). Age differences of less than 2 billion years in intermediate-metallicity clusters are adequate to produce the range of HB morphologies observed among such clusters, as could a range in helium of $\Delta Y = 0.03$, in CNO/Fe, or in mean stellar rotation. Peterson (1984) has recently presented observational evidence in support of the hypothesis that rotation is an important factor in HB morphology, while Searle and Zinn (1978), among others, have argued that age differences are the dominant factor.

As we have seen above, such a small range in age is extremely difficult to rule out, given uncertainties in metallicity (and reddening when it is somewhat larger than in the present cases) and photometric uncertainties arising largely from crowding problems.

IV. STAR COUNTS

Star counts as a function of distance from the cluster center in a globular cluster can be used to derive its tidal radius, which in turn can constrain the potential field in the outer halo of the Galaxy and the cluster's orbit. Peterson and King (1975) discuss the theoretical and observational techniques for determining tidal radii as applied to photographic data.

To facilitate star counts, each frame was taken with the center of the cluster slightly offset from the center of the frame. Thus, although the 4 shooter field is a square whose sides are 8.9 arcmin, star counts could be obtained to radii of almost 7 acmin with two of the chips having good coverage of the central region of the cluster, and the two others covering the periphery of the cluster. Thus, for example, full annular coverage for NGC 6229 is available for $r \leqslant 145$ arcsec, and coverage over more than 85% of the full annulus is available for $r \leqslant 240$ arcsec. More than one quarter of the full annulus is present for $r \leqslant 380$ arcsec, which is close to the largest radius for which counts are actually given here. Similar, but not identical, fractions of areal coverage as a function of radius hold for NGC 7006.

The same point-source-detection software described in Sec. II was used on the 600 s g exposures to generate star counts as a function of radius from the cluster center, but the threshold for detection was set somewhat higher (equivalent to $g \leqslant 23.4$ mag) than that used for the color-magnitude diagrams. The area within 0.5 arcmin of the cluster center was ignored, but otherwise the whole area of each chip was surveyed for point sources. 1931 point sources were detected in NGC 7006 and 2528 in NGC 6229 above the threshold level and below the saturation level of the detector. NGC 5466 is too extended to reach the background field within a single 4-Shooter frame, and we do not present any such data for this cluster. The number of detected stars within each chip as a function of radius was corrected for the fraction of the annulus at each radius that was missing from that particular chip to derive the final stellar surface densities. The counts for each chip were kept separately, although each is scaled to full areal coverage. The stellar surface density became approximately constant beyond $r = 5.3$ arcmin in both clusters, and the mean value at larger r was taken to be the background value. (This may slightly overestimate the background; ideally it should be determined at even larger radii.) The star counts, corrected for the background, for NGC 6229 and NGC 7006 are presented in Fig. 13, where the stellar surface density (f) is given in units of stars per 100 arcsec^2. Each of the four chips is plotted at all radii for which data were available, with a correction factor for missing area of less than 25. There is no separation in Fig. 13 between the individual chips. However, it is apparent from examining the locations of the detected objects superposed on an image of each cluster that the counts in the innermost region are underestimated due to crowding. This effect is also clearly visible in the figure.

King *et al.* (1968) published visual star counts for these two clusters, which were used by Peterson and King (1975) to derive their tidal radii. The limiting magnitude of the photographic plates used for NGC 6229 was about 21 in B (although one should not imagine good efficiency in visually counting stars down to the plate limit), and a total of 1197 stars were counted, many of which would be too bright to be included in our counts. Less than 650 stars were counted in NGC 7006. Their star counts do not extend out to larger radii from the cluster center than those given here. To directly compare the two data sets, we have scaled King *et al.*'s star counts to ours by the ratio of the background values adopted by King *et al.* (1968) to those we choose for each of the clusters. (An error in the scaling, perhaps due to a variation of the luminosity function of the background field with respect to the cluster stars, would uniformly shift the King *et al.* curve vertically in Fig. 13.) The resulting scaled counts from King *et al.* (1968) are plotted in Fig. 13 as light circles. The comparison is somewhat sobering, especially when one realizes that our most likely error is an overestimation of the background, which would uniformly lower vertically the light circles representing the King *et al.* counts in Fig. 8, and would underestimate the stellar density for our counts by the amount the background was underestimated, an effect particularly important in the outermost parts of each cluster.

NGC 6229 is clearly as large as our star counts indicate.

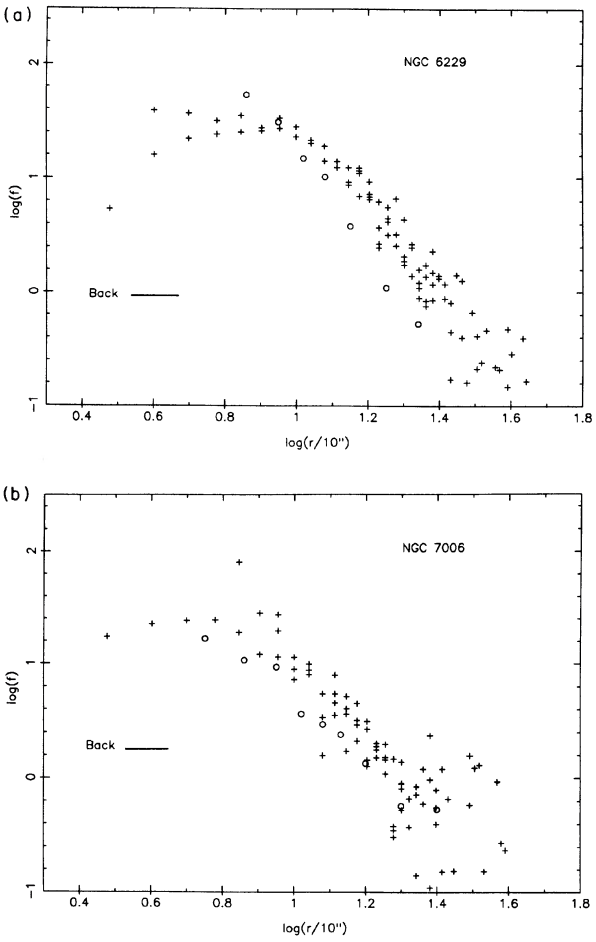

FIG. 13.(a),(b) The surface density of stars in NGC 6229 and NGC 7006 corrected for a background stellar density is shown as a function of distance from the cluster center. The crosses represent the corrected results for each individual 4-Shooter chip. The background subtracted is indicated by the solid horizontal line. The light circles represent the counts of King *et al.* (1968) scaled to the same background stellar density.

The most distant corner of Field 5 in NGC 6229, shown in Fig. 2, is 275 arcsec from the cluster center. Nearly all of the stars in this field fit onto the cluster c-m diagram and hence must be cluster members. This radius is beyond the outer edge of the outermost annulus of the King *et al.* counts. In NGC 6229, one sees a clear hint that the manual counts from photographic plates had a systematic dependence of the magnitude range included with radius, so that the spatial extent of the cluster was underestimated. It is of course also possible that the differences in radial distribution are due to mass segregation; the sense of the difference is correct since the King *et al.* (1968) counts included mostly giants, while ours are dominated by stars of somewhat lower mass. However, a similar analysis of the giants in NGC 6229 from our 136 s *g* 4-Shooter frame using a bright magnitude cutoff led to radial distributions for 343 stars. These giants showed the same radial distribution as did the fainter stars, although they did not show the rolloff due to crowding in the central area as severely as did the faint star counts. It is thus likely that the older star-count data are faulty, and that the tidal radius of NGC 6229, in particular, has been underestimated.

V. SUMMARY

Color-magnitude diagrams of three distant galactic globular clusters (NGC 5466, 6229, and 7006) have been given in the Thuan-Gunn *g,r* photometric system, and transformed to the Johnson *B,V* system. The magnitudes are measured in boxes 1.65 arcsec on a side centered on each point source; offsets determined from well-isolated stars are used to convert the box magnitudes to large-aperture photometry. The photometry reaches below the main-sequence turnoff in all three clusters. Comparison with the isochrones of VandenBerg (1983) and of VandenBerg and Bell (1984) demonstrate that the ages of these three clusters are indistinguishable from those of the better-studied nearby globular clusters; the claims of Carney and Inman (1982) and Carney (1984) of an exceptionally bright turnoff in NGC 7006 are spurious.

Computer-generated star counts given in Sec. III*b* for the three clusters are used to generate luminosity functions by patching together counts in the crowded inner regions, which contain many bright stars, and in the outlying fields, where the limiting magnitude is deeper. The luminosity functions indicate that the maximum difference in age between NGC 5466 and NGC 6229 is $\pm$ 10% of the age, while it is $\pm$ 25% for NGC 5466 and NGC 7006.

The horizontal branch of NGC 6229 is unusually red; it is an even more extreme example of the second parameter problem than NGC 7006. The predicted differences in age between globular clusters that are required to produce the observed variations in horizontal-branch morphology (i.e., the second parameter effect) are too small to be detected in the present data.

NGC 6229 is more extended than was found from King *et al.*'s (1968) visual star counts. The tidal radius for NGC 6229 obtained by Peterson and King (1975) from the old star-count data is also probably somewhat underestimated.

This research was supported by NSF Grant No. AST 82-12270. I am grateful to Alain Porter for a useful software routine, and especially to Keith Shortridge, who wrote the basic image-processing software package in use at Caltech. To Jim Gunn and the entire crew who built the 4-Shooter—bravissimo. I also thank the referee for critical and thoughtful comments on the original version of this manuscript that forced me not to be lazy.

REFERENCES

Baade, W. (1945). Astrophys. J. **102**, 17.
Blanco, V. M., Demers, S., Douglass, G. G., and Fitzgerald, M. P. (1968). Publ. U. S. Naval Obs. **21**, 1968.
Buonanno, R., Buscema, G., Corsi, C. E., Iannicola, G., and Fusi-Pecci, F. (1984). Astron. Astrophys. Suppl. **56**, 79.
Burstein, D., and Heiles, C. (1983). Astrophys. J. Suppl. **54**, 33.
Carney, B. W. (1984). Publ. Astron. Soc. Pac. **96**, 841.
Carney, B. W., and Inman, R. T. (1982). Bull. Am. Astron. Soc. **14**, 878.
Cohen, J. G., and Frogel, J. A. (1982). Astrophys. J. Lett. **255**, L39.
Cuffey, J. (1961). Astron. J. **66**, 71.
Flannery, B. P., and Johnson, B. C. (1982). Astrophys. J. **263**, 166.
Freeman, K. C., and Norris, J. (1981). Annu. Rev. Astron. Astrophys. **19**, 319.
Frogel, J. A., Cohen, J. G., and Persson, S. E. (1983). Astrophys. J. **275**, 773.

Gunn, J. E., Carr, M., Chang, J., Danielson, G. E. A., Lorenz, E. O., Lucinio, R., Nenow, V. E., Smith, O. J., Westphal, J. A., and Zimmerman, B. A. (1984). Bull. Am. Astron. Soc. **16**, 447.
Harris, W. E., and Racine, R. (1979). Annu. Rev. Astron. Astrophys. **17**, 241.
Iben, I., Jr. (1971). Publ. Astron. Soc. Pac. **83**, 697.
Kent, S. M. (1985). Publ. Astron. Soc. Pac. **97**, 165.
King, I. R., Hedemann, E., Jr., Hodge, S. M., and White, R. E. (1968). Astron. J. **73**, 456.
Paczynski, B. (1984). Astrophys. J. **284**, 670.
Peterson, C. J., and King, I. R. (1975). Astron. J. **80**, 427.
Peterson, R. (1984). Astrophys. J. Lett. **294**, L35.
Renzini, A. (1977). In *Advanced Stages of Stellar Evolution*, edited by P. Bouvier and A. Maeder (Geneva Observatory, Geneva), p. 151.
Sandage, A. R. (1970). Astrophys. J. **162**, 841.
Sandage, A. R., and Wildey, R. (1967). Astrophys. J. **150**, 469.
Schneider, D. P., and Gunn, J. E., and Hoessel, J. G. (1983). Astrophys. J. **264**,337.
Searle, L., and Zinn, R. (1978). Astrophys. J. **225**, 357.
Thuan, T. X., and Gunn, J. E. (1976). Publ. Astron. Soc. Pac. **88**, 543.
VandenBerg, D. A. (1983). Astrophys. J. Suppl. **51**, 29.
VandenBerg, D. A., and Bell, R. A. (1985). Astrophys. J. Suppl. **58**, 561.
Zinn, R. J. (1980). Astrophys. J. Suppl. **42**, 19.